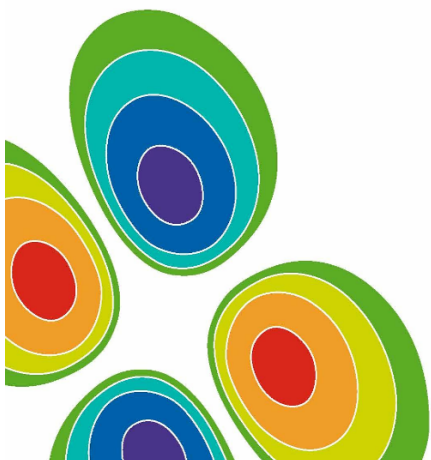




Magnetism at the Edge; New phenomena at oxide interfaces

J. M. D. Coey

School of Physics and CRANN
Trinity College Dublin, Ireland.



J. M. D. Coey, Ariando, W. E. Pickett, MRS Bulletin, 38 1040 (2013)

Zug 15-viii-2014

Magnetism at the edge

Three short stories

J. M. D. Coey

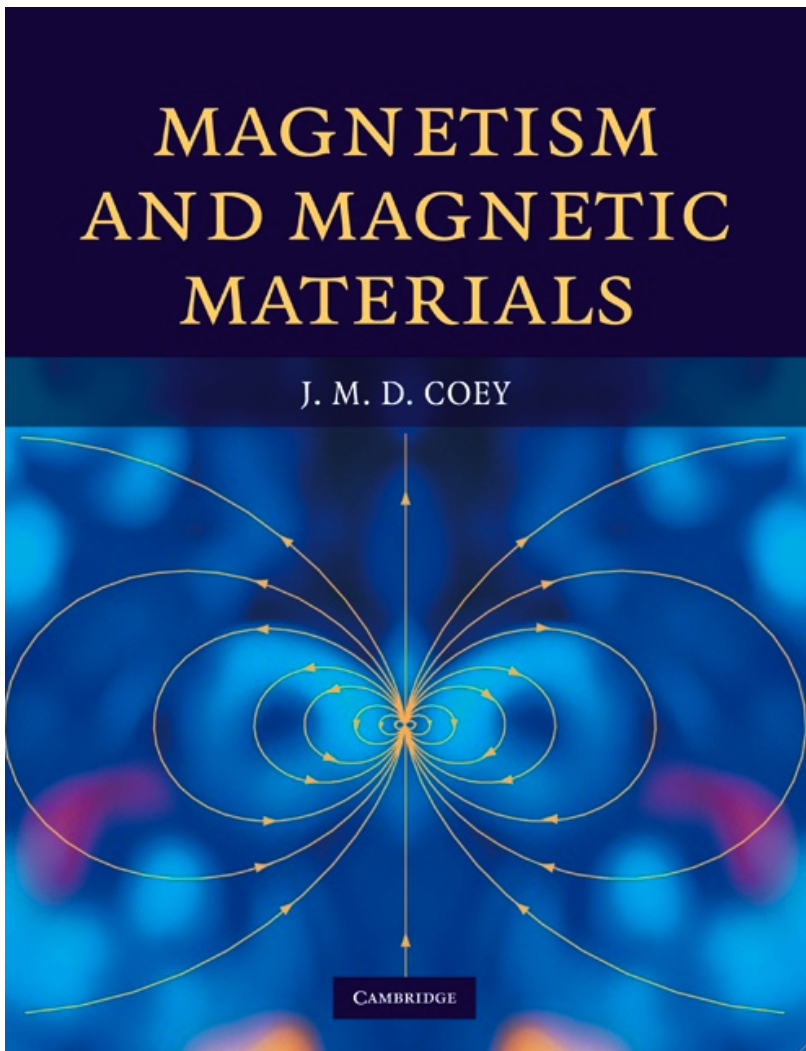
Introduction - Magnetic thin films

1. MRG-The zero-moment half metal
2. Playing with the polar catastrophe
3. d^0 magnetism



www.tcd.ie/Physics/Magnetism

Zug 15-viii-2014



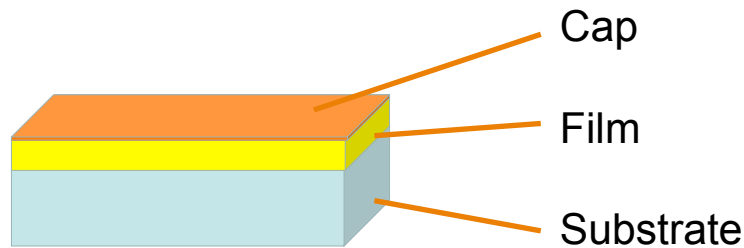
CUP 2010 Cost ~ €50

www.cambridge.org/9780521816144

- 1 Introduction
- 2 Magnetostatics
- 3 Magnetism of the electron
- 4 The many-electron atom
- 5 Ferromagnetism
- 6 Antiferromagnetism and other magnetic order
- 7 Micromagnetism
- 8 Nanoscale magnetism
- 9 Magnetic resonance
- 10 Experimental methods
- 11 Magnetic materials
- 12 Soft magnets
- 13 Hard magnets
- 14 Spin electronics and magnetic recording
- 15 Other topics
- Appendices, conversion tables.

Introduction - Magnetic thin films

Magnetic thin films



Achievable sensitivity with SQUID magnetometer 10^{-11} Am^2

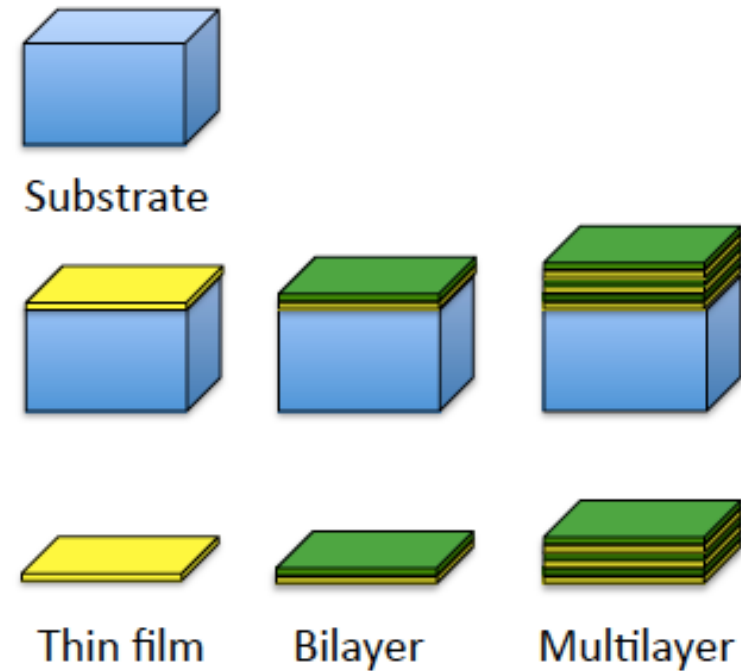
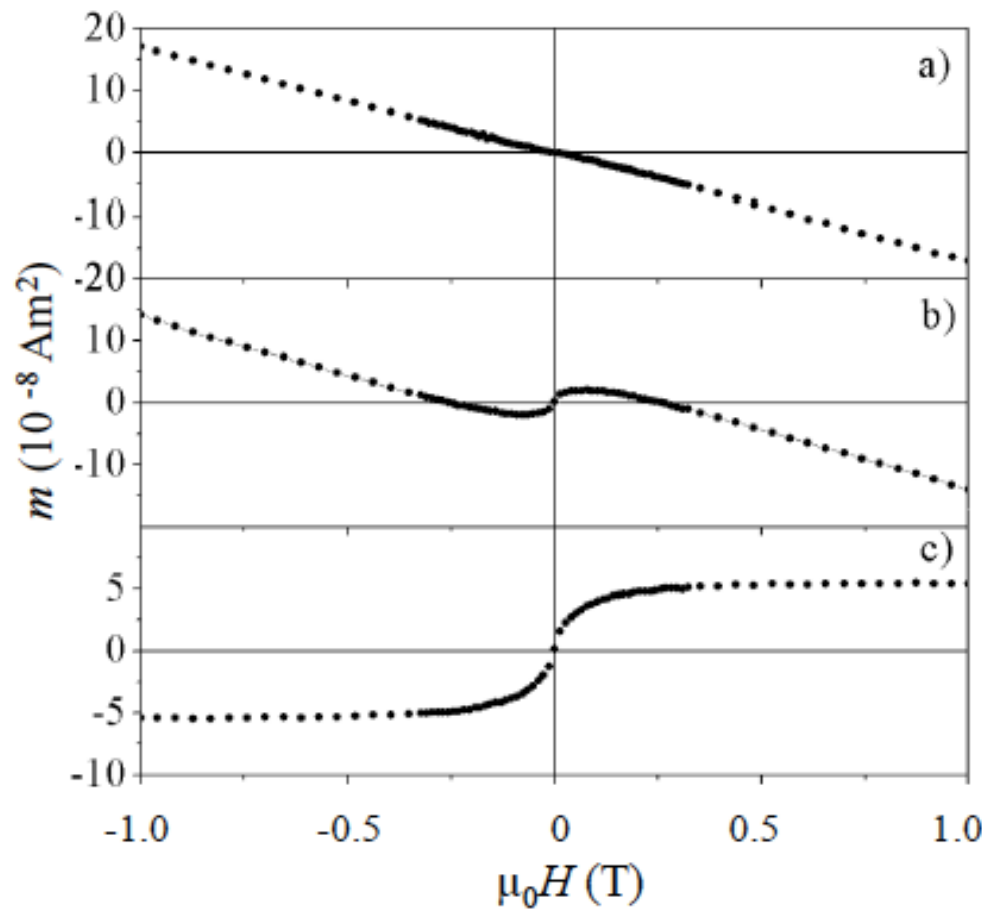
Ferromagnetic monolayer $5 \times 5 \text{ mm}^2$ $\sim 10^{-8} \text{ Am}^2$

Moment of oxide substrate $5 \times 5 \times 0.5 \text{ mm}^2$ in 1 MAm^{-1} $\sim 10^{-8} \text{ Am}^2$

Table I. Magnetic susceptibility of insulating oxides. Units (SI) are 10^{-6} .

Al_2O_3	MgO	SrTiO_3	LaAlO_3	TiO_2	SiO_2	YSZ	MgAl_2O_4
-18	-11	-7	-18	4	-18	-8	-15





Assume $m_{\text{sample}} = m_{\text{sample on substrate}} - m_{\text{substrate}}$

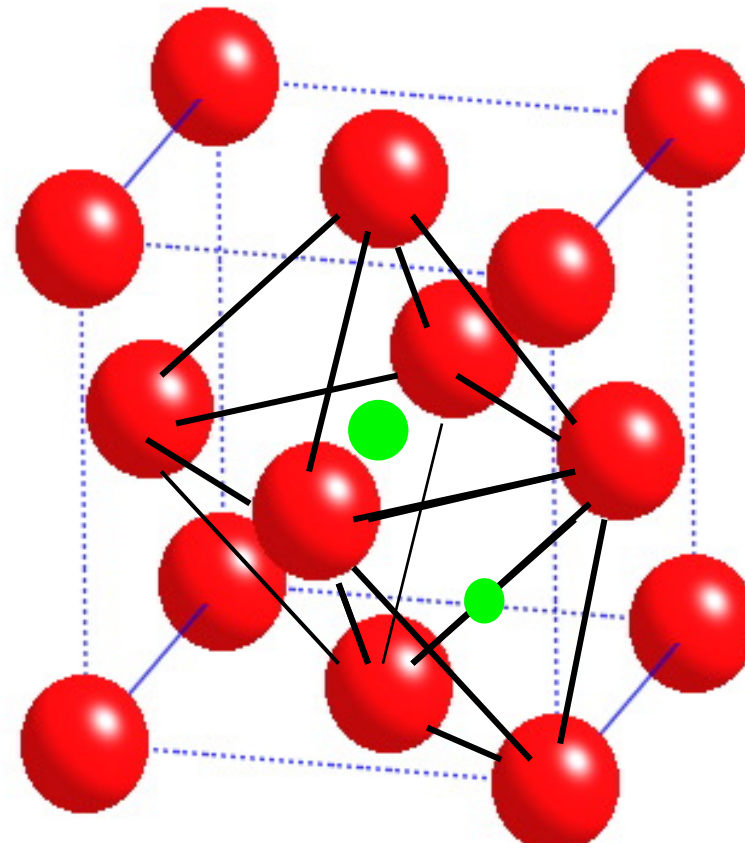
This could be naïve

Substrates

Substrate	a, c (pm)
Al_2O_3	477, 1304
MgO	420
SrTiO_3	391
LaAlO_3	379
TiO_2	459,296
SiO_2	490,539
YSZ	513
MgAl_2O_4	808

Scope for exerting biaxial strain, and growing otherwise unstable materials.

Oxides are usually insulating.
Structures are based on dense-packed O^{2-} arrays, with cations in interstitial sites.

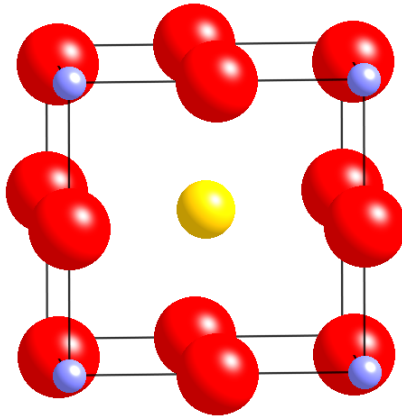


$$R_{\text{oct}} = (\sqrt{2}-1)r_{\text{O}} = 58 \text{ pm}$$

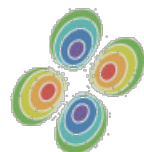
Zug 15-viii-2014

$$R_{\text{tet}} = (\sqrt{(3/2)} - 1)r_{\text{O}} = 32 \text{ pm}$$





Perovskite structure
 ABO_3



MAGNETISM &
 SPIN ELECTRONICS
 TRINITY COLLEGE, DUBLIN

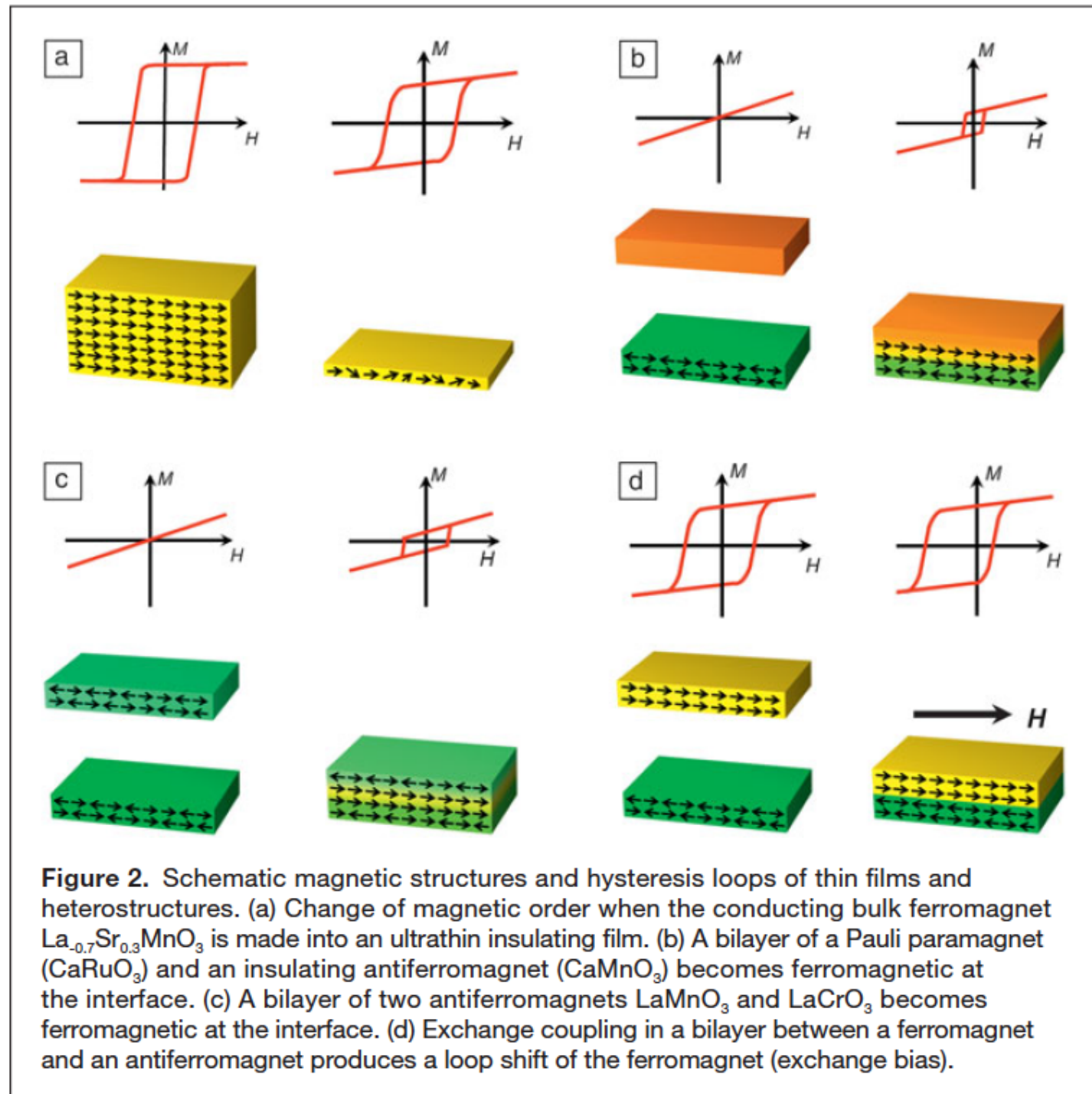


Figure 2. Schematic magnetic structures and hysteresis loops of thin films and heterostructures. (a) Change of magnetic order when the conducting bulk ferromagnet $\text{La}_{0.7}\text{Sr}_{0.3}\text{MnO}_3$ is made into an ultrathin insulating film. (b) A bilayer of a Pauli paramagnet (CaRuO_3) and an insulating antiferromagnet (CaMnO_3) becomes ferromagnetic at the interface. (c) A bilayer of two antiferromagnets LaMnO_3 and LaCrO_3 becomes ferromagnetic at the interface. (d) Exchange coupling in a bilayer between a ferromagnet and an antiferromagnet produces a loop shift of the ferromagnet (exchange bias).

1. MRG - A zero-moment half metal

H. Kurt, K Rode, Y. C. Lau, N. Thiyanarajah, P. Stamenov, J. M. D. Coey

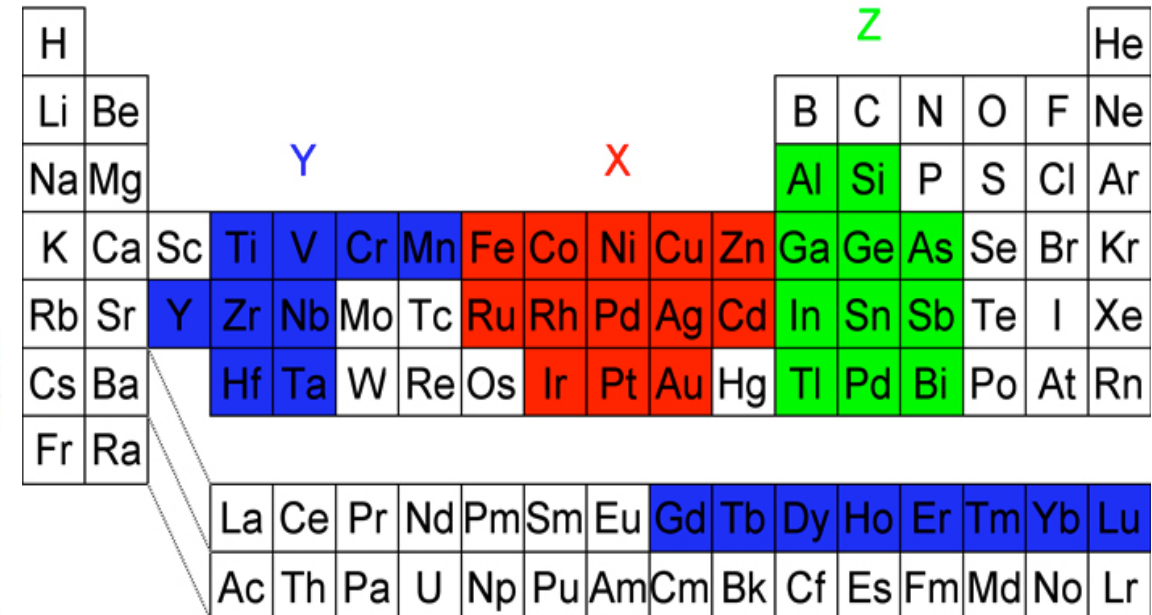
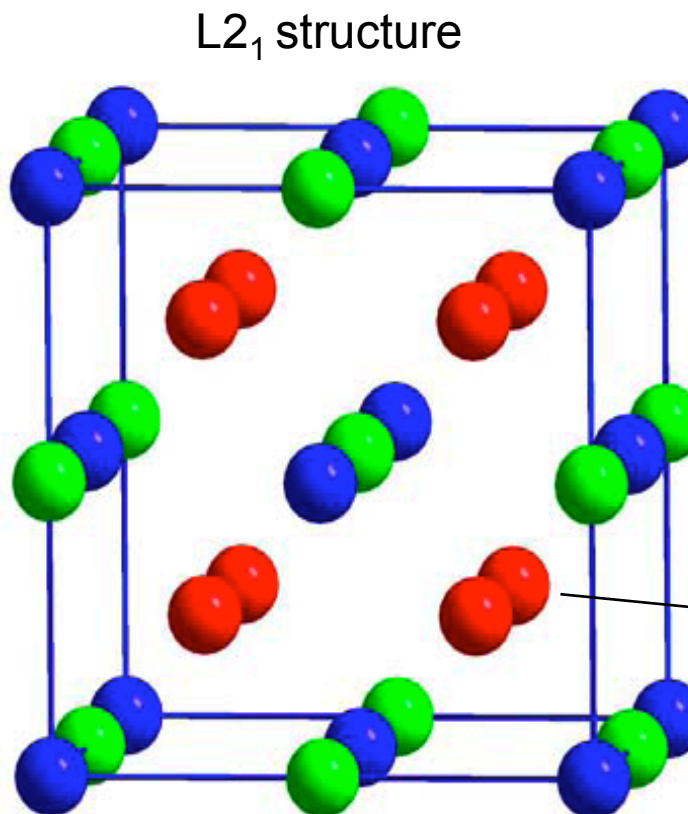


H Kurt et al PRL 112 027201 (2014)

Zug 15-viii-2014

Heusler Alloys X_2YZ

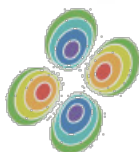
Cubic L₂₁ structure



Co₂MnSi Co₂FeSi

$T_c = 985 \text{ K}$ $T_c = 1120 \text{ K}$
 Mn

Zug 15-viii-2014



$$m = n_{\uparrow} - n_{\downarrow}$$

$$n_{tot} = n_{\uparrow} + n_{\downarrow}$$

$$m = n_{tot} - 2n_{\downarrow}$$

$$n_{\downarrow} = 12$$

$m = n_{tot} - 24$

$$m = n_v - 2n_{\downarrow}$$

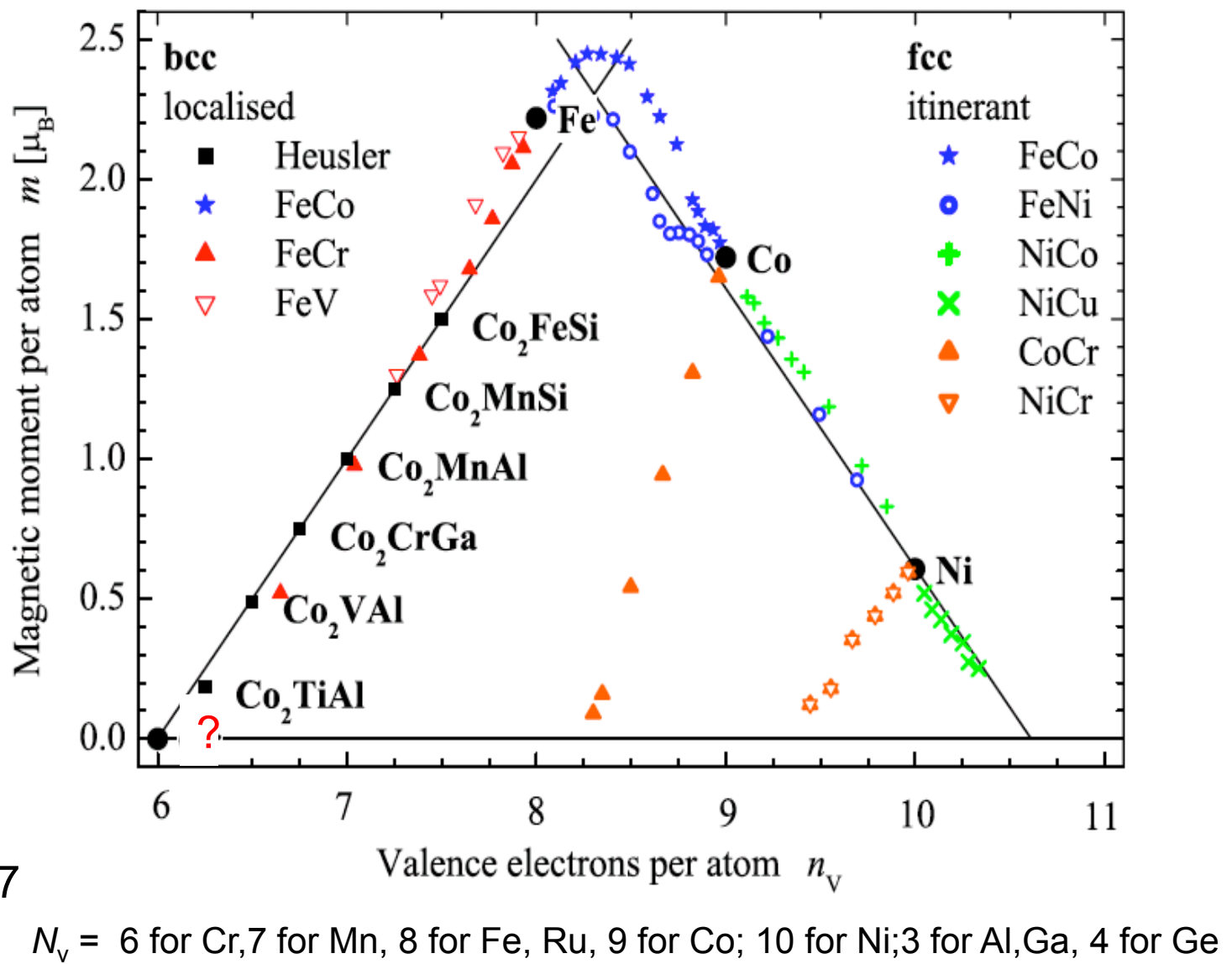
or

$$m = 2n_{\uparrow} - n_v$$

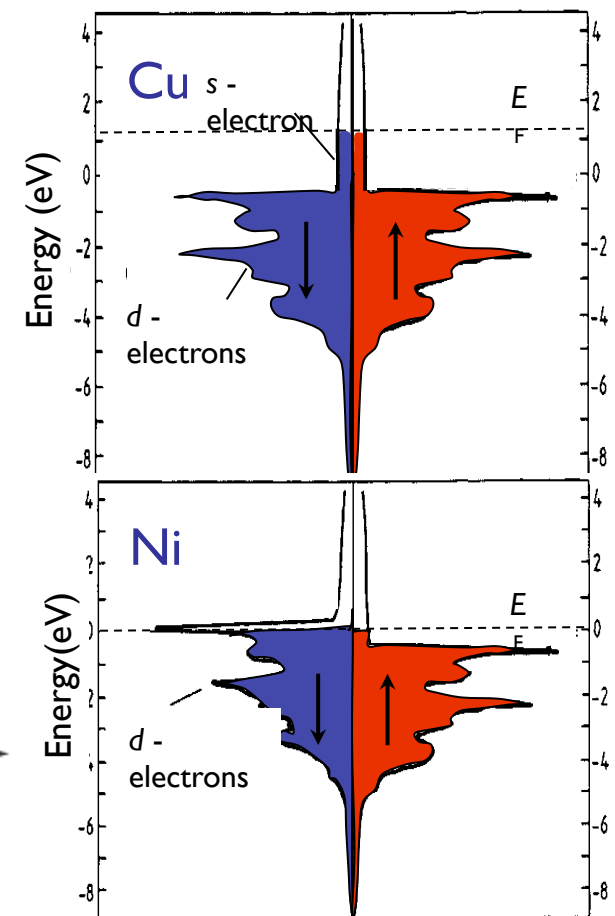
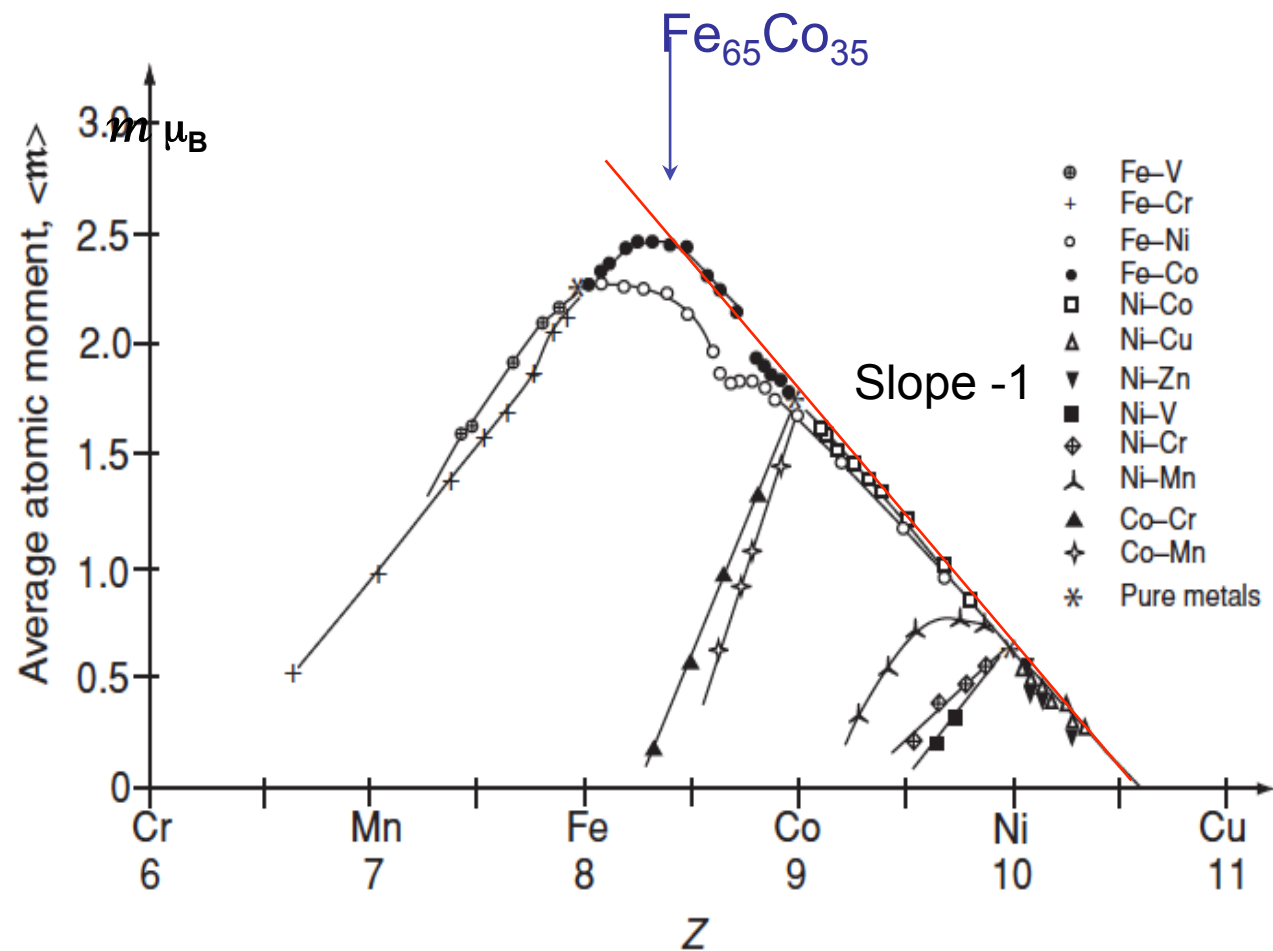
e.g. Co_2CrAl

$$2 \times 9 + 6 + 3 = 27$$

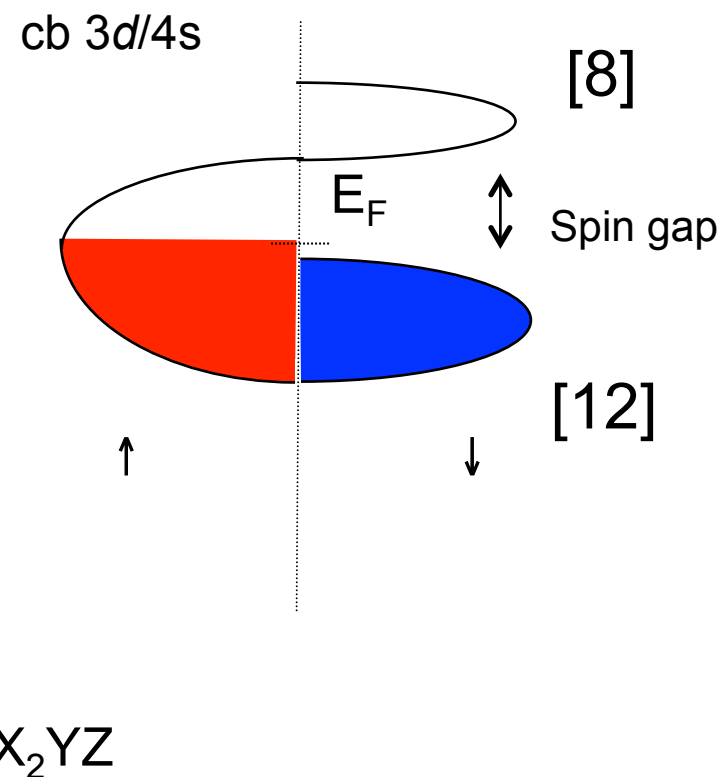
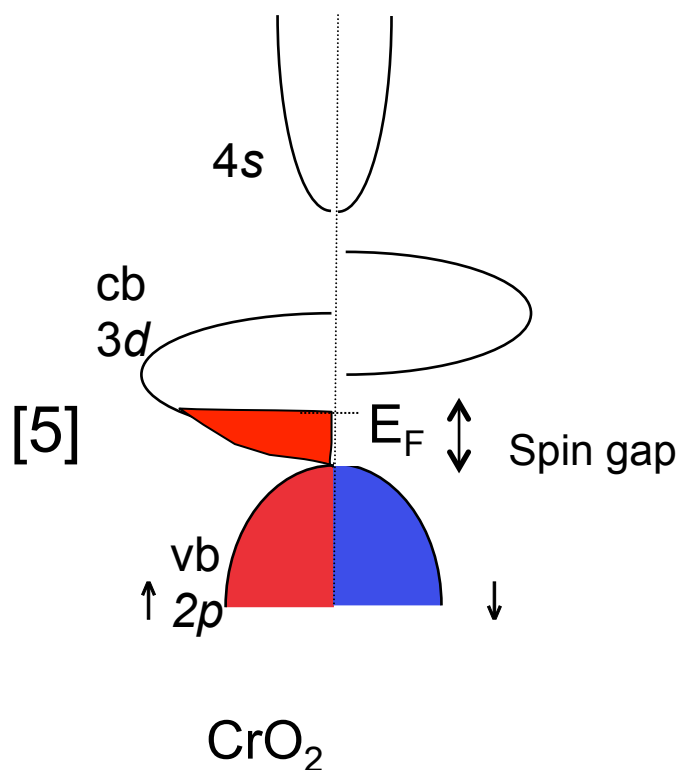
$$m. = 3\mu_B$$



Slater-Pauling Curve



A half-metal



$$m = n_{\uparrow} - n_{\downarrow}$$

$$n_{tot} = n_{\uparrow} + n_{\downarrow}$$

$$m = n_{tot} - 2n_{\downarrow}$$

$$n_{\downarrow} = 12$$

$m = n_{tot} - 24$

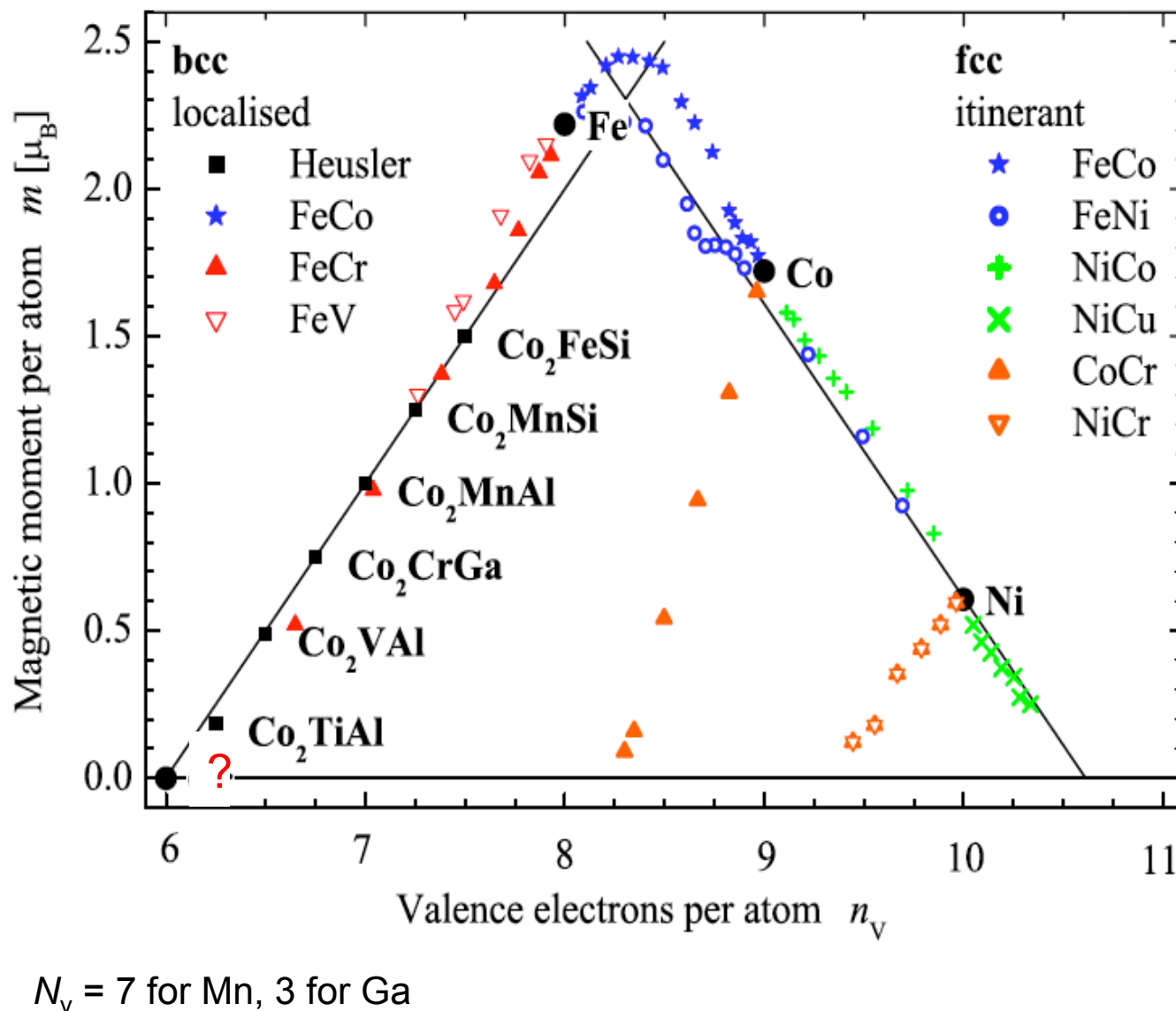
$$m = n_v - 2n_{\downarrow}$$

or

$$m = 2n_{\uparrow} - n_v$$

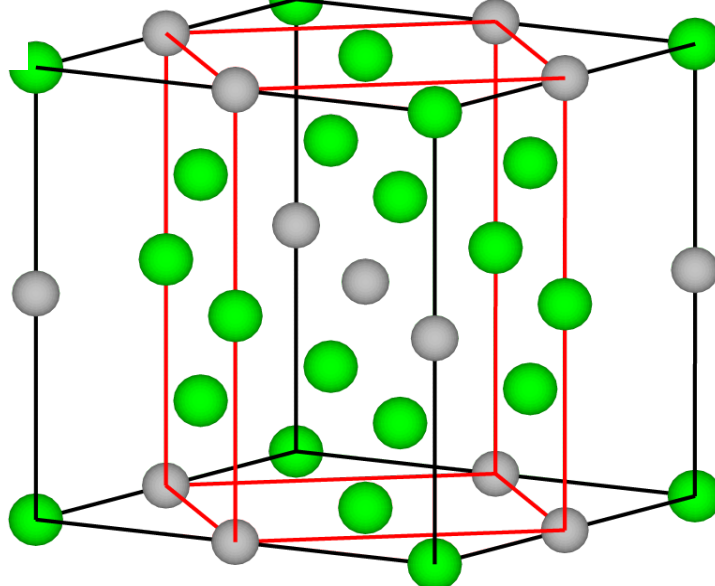
e.g. Mn_3Ga
 $3 \times 7 + 3 = 24$

$$m = 0 \mu_B$$



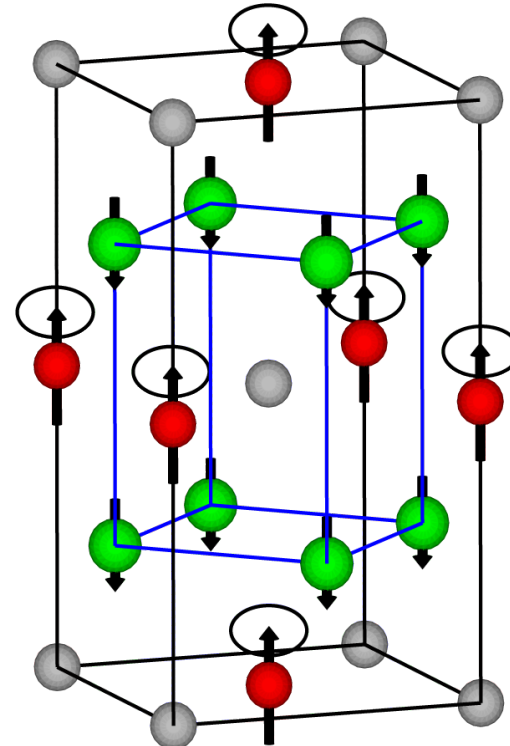
Mn₃Ga

Cubic $D0_3$ X₂YZ Heusler; X = Y



Ordered bcc

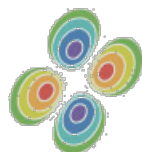
Tetragonal $D0_{22}$



$$m = 1.1 \mu_b/\text{f.u}$$

Ordered fct

c-axis extension $\approx 20\%$



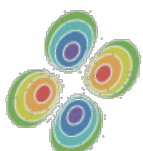
Mn_{3-x}Ga thin film growth

In-plane lattice spacings (Angstroms) for various substrates and seed layers

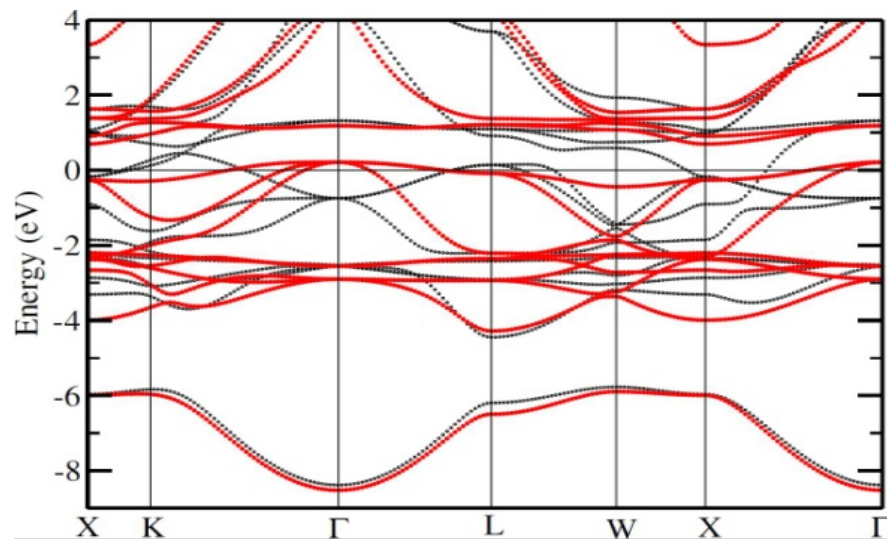
InAs †	4.28	AlAs †	4.00
V*	4.28	Pt	3.92
MgO	4.21	SrTiO ₃	3.90
Cr*	4.11	Pd	3.89
Au	4.08	Ru	3.82
Al	4.05	Si †	3.84
GaAs †	4.00	Cu	3.61

* $a_0\sqrt{2}$ † $a_0/\sqrt{2}$ Mn₃Ga (D0₂₂) a = 3.92 Å;

Mn₃Ga (D03) $a_0/\sqrt{2} = 4.22$ Å

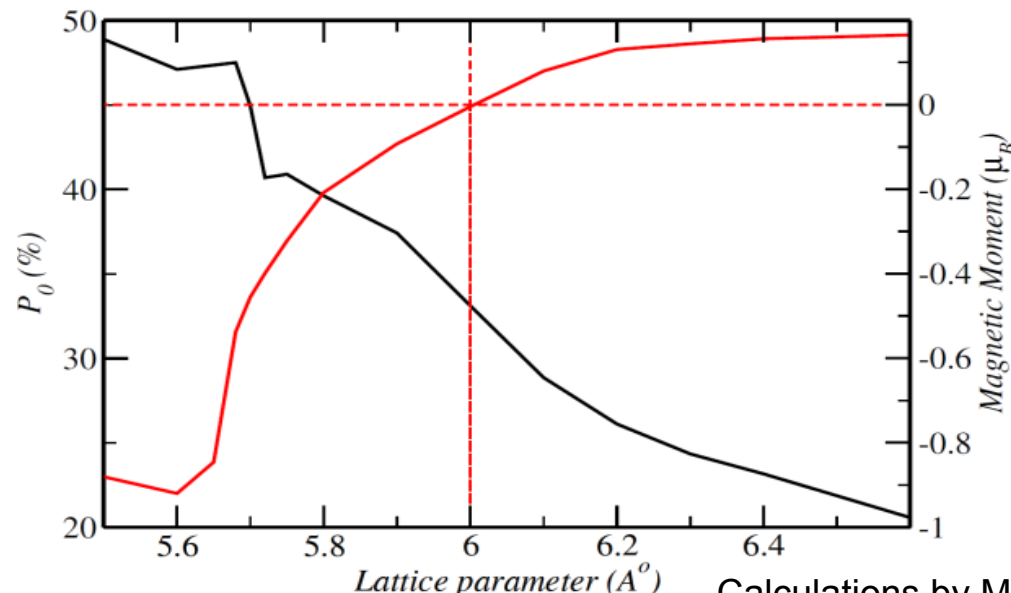


Electronic structure of cubic Mn_2Ga films



Note the spin gap 0.2 eV above E_F

Type/Magnetic configuration	Ferromagnetic	Antiferromagnetic
Type I, MnGaMn or MnMnGa	842	0
Type II, GaMnMn	187	68

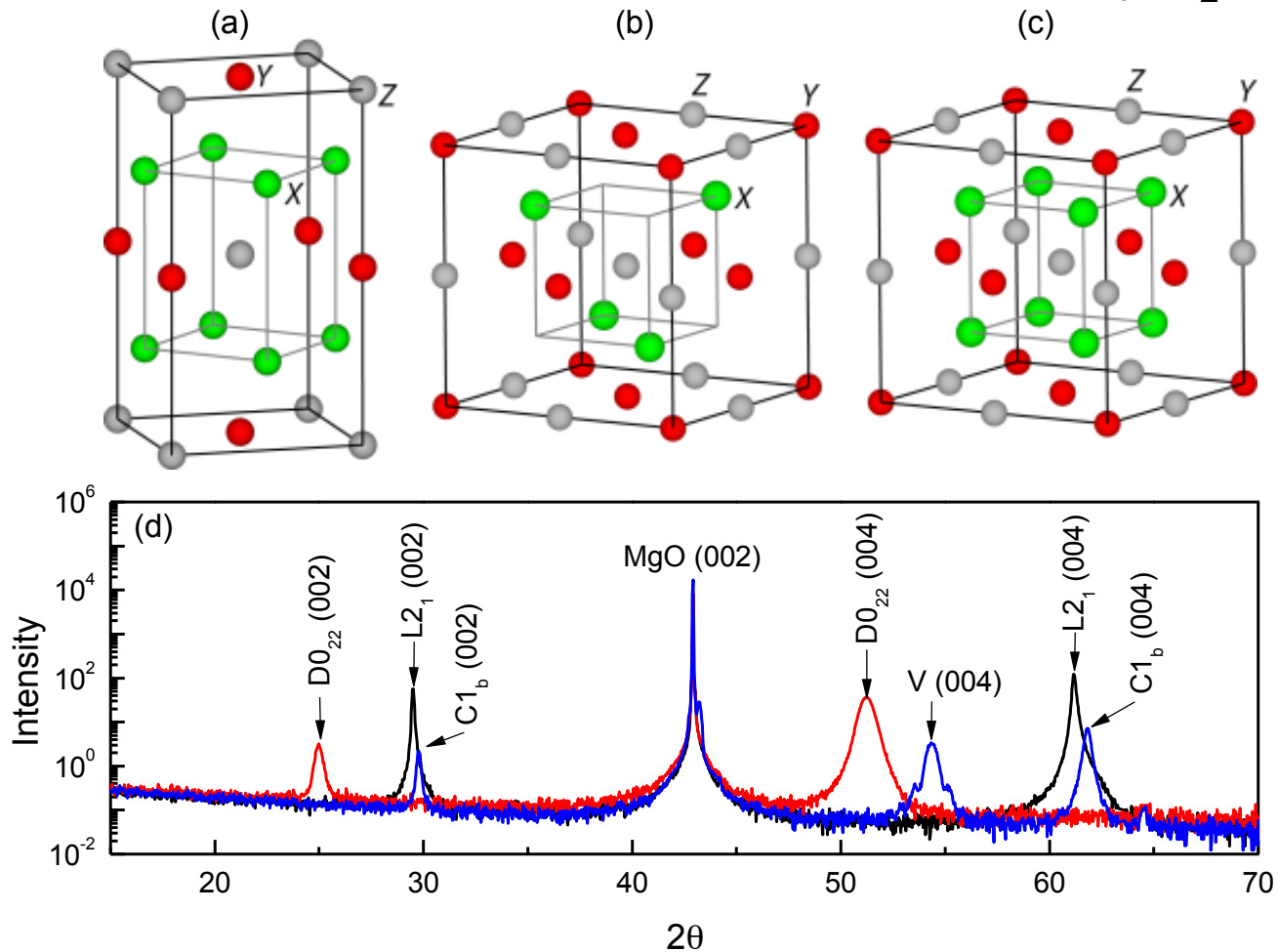


Growth of cubic Mn_3Ga and Mn_2Ga films

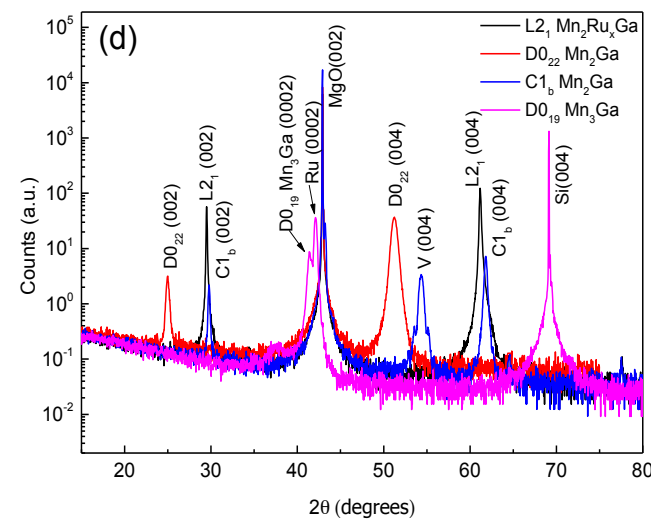
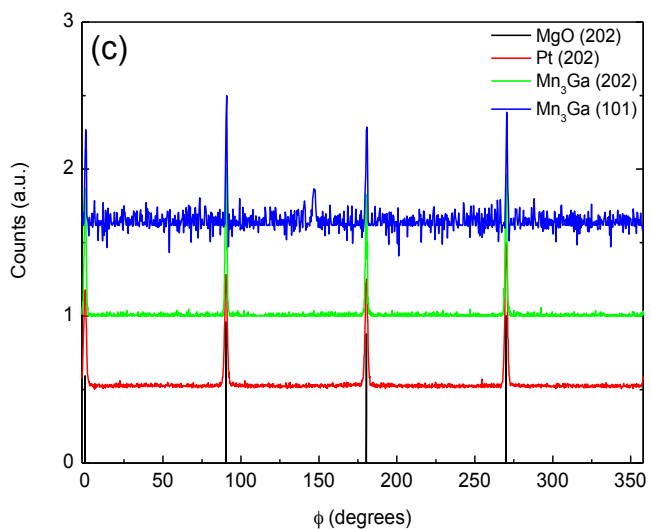
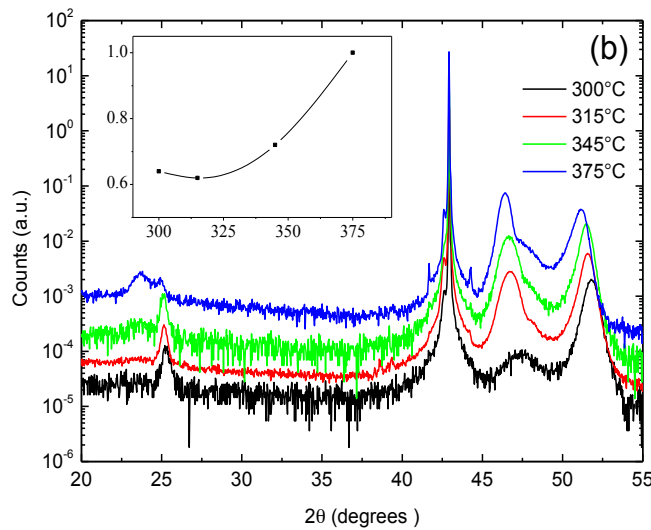
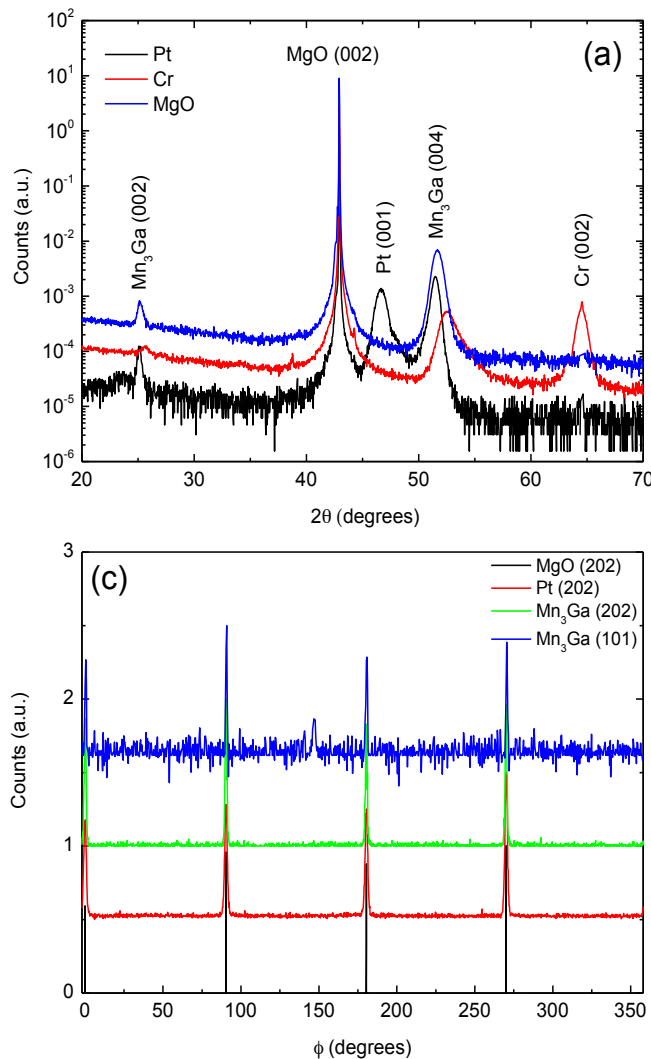
$$m(\text{Mn}_3\text{Ga}) = 0.5\mu_B/\text{fu}$$

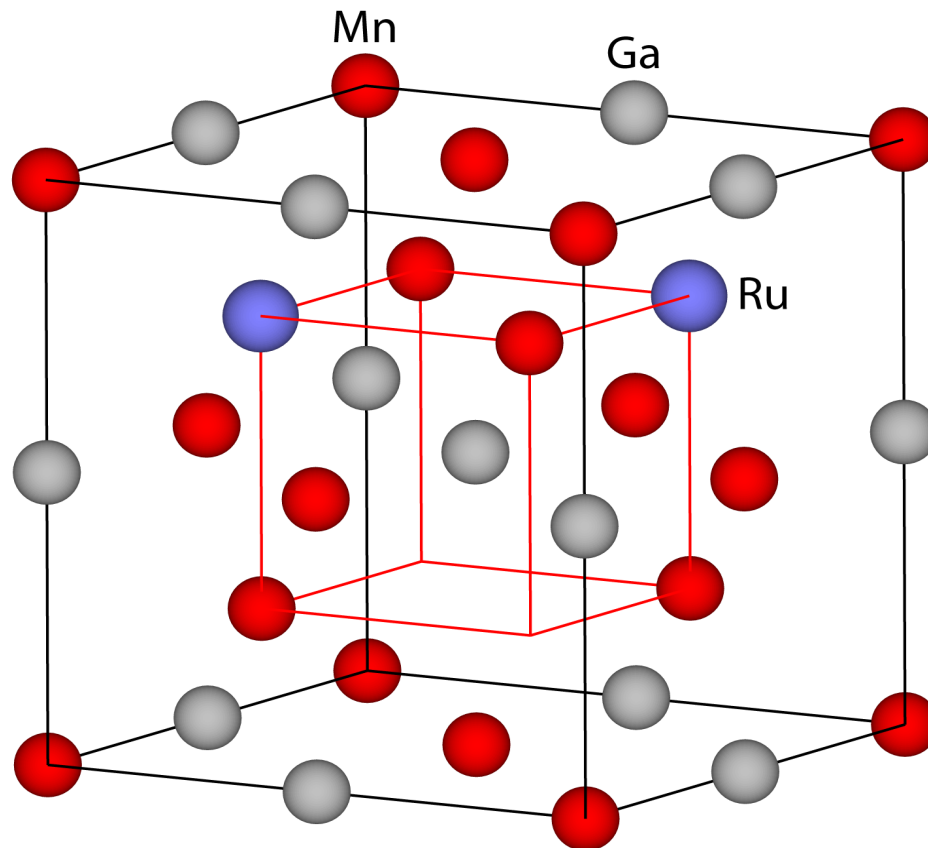
$$m(\text{Mn}_2\text{Ga}) = (-)1.6\mu_B/\text{fu}$$

$$m(\text{Mn}_2\text{RuGa}) = 0.6\mu_B/\text{fu}$$



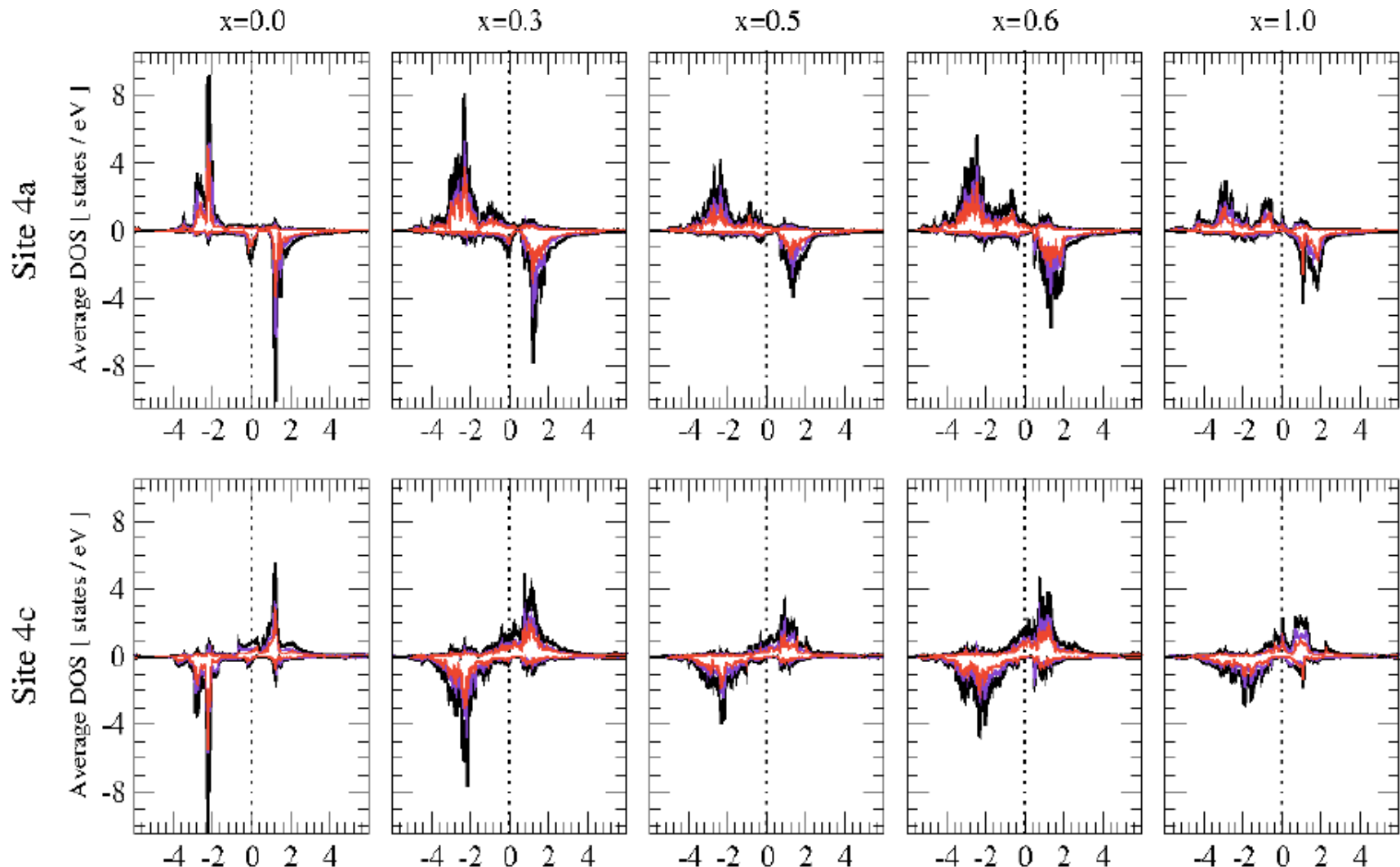
Mn₂Ru_xGa films; Cubic with biaxial strain





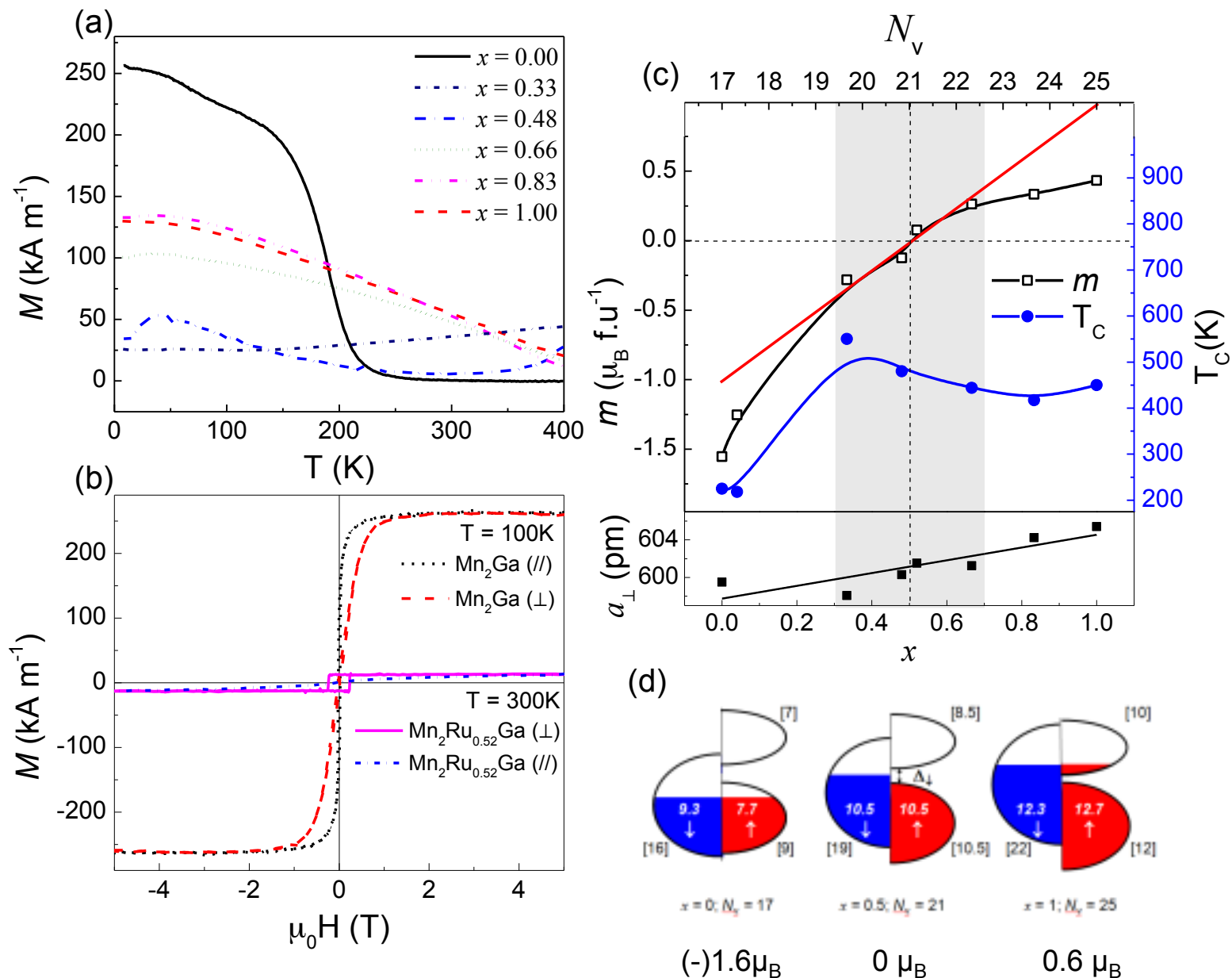
Atomic structure of cubic $\text{Mn}_2\text{Ru}_{0.5}\text{Ga}$ MRG $n_v = 18$

Ruthenium occupies half of the 4d sites and there are no Ru-Ga nearest neighbours.

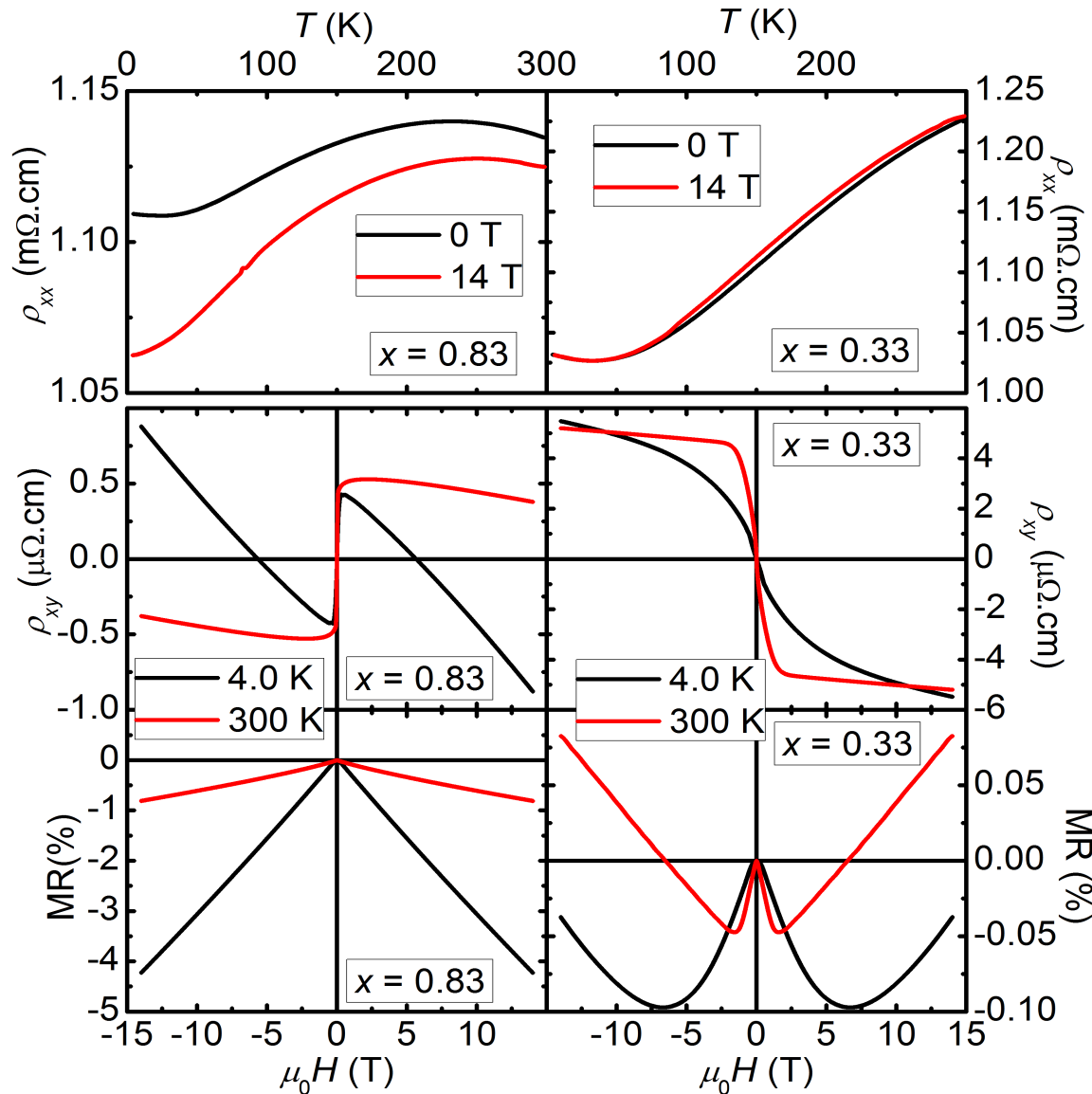


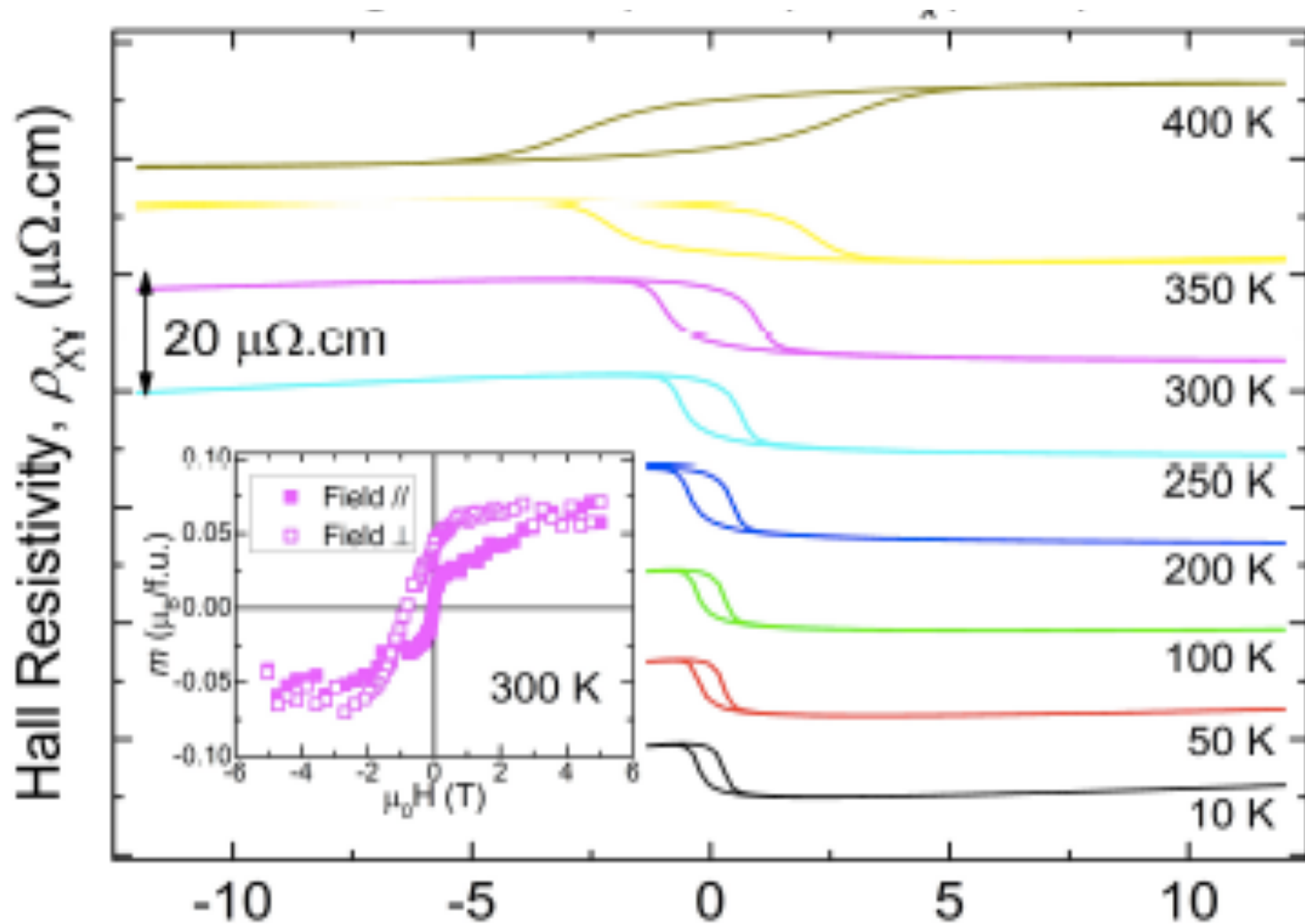
Calculations by Mario Zic, Stefano Sanvito

Zug 15-viii-2014

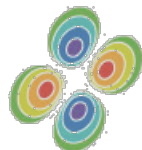


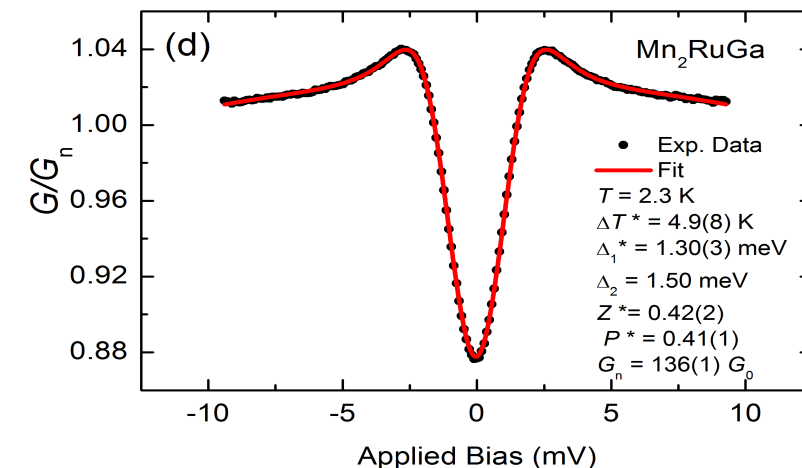
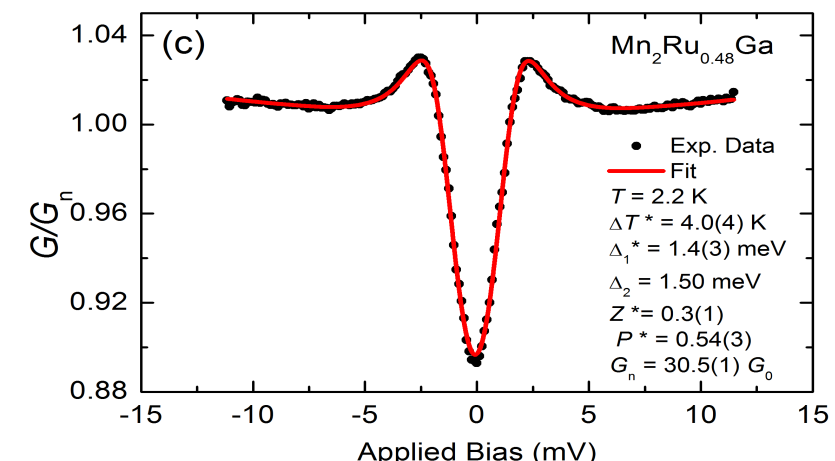
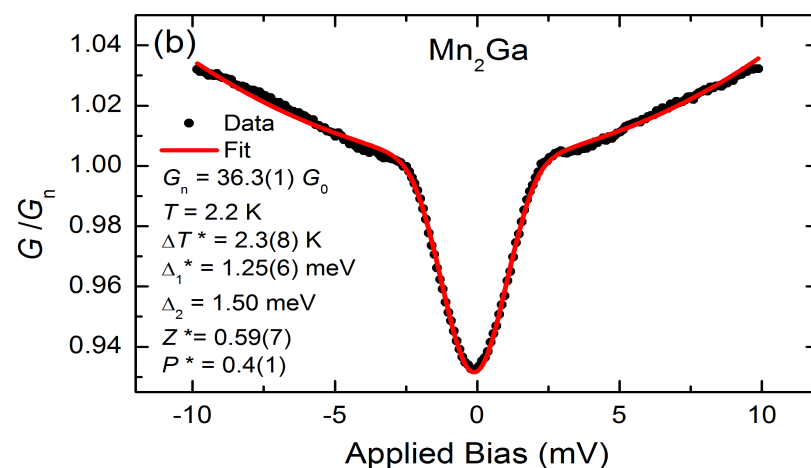
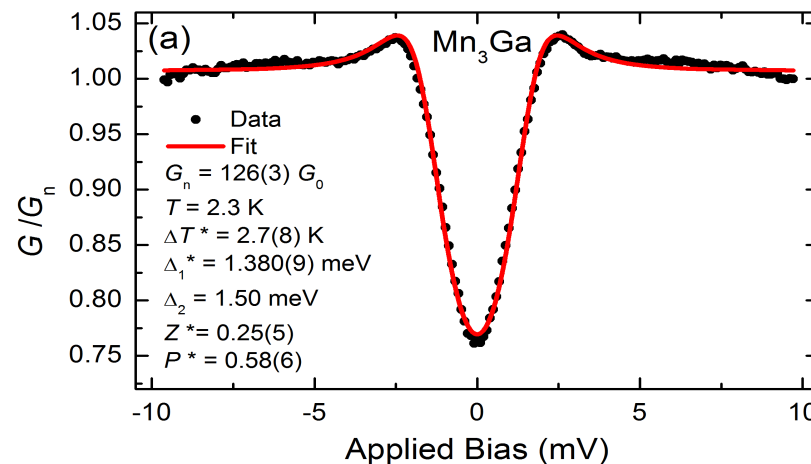
Magnetotransport properties of cubic $\text{Mn}_2\text{Ru}_x\text{Ga}$ films





The two sublattices have different temperature dependence





PCAR Summary



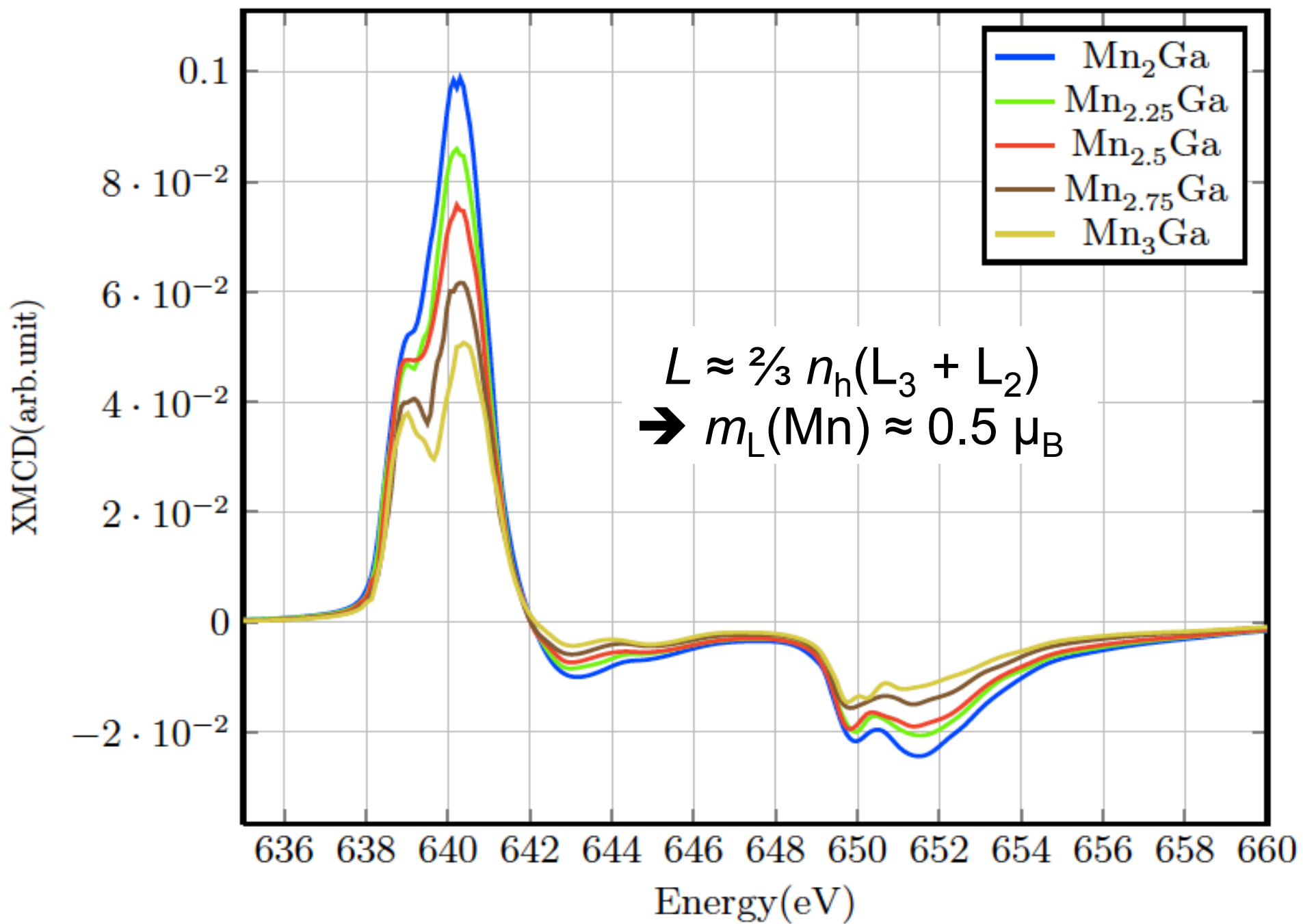
MAGNETISM &
SPIN ELECTRONICS
TRINITY COLLEGE, DUBLIN

Film stack	Spin Polarization (%)	Resistivity ($\mu\Omega\text{cm}$)	Magnetization (kA m^{-1})
Pt/ Mn_3Ga ⁶²	58	160	110
MgO/ Mn_2Ga ⁶¹	40	120	470
SrTiO ₃ / Mn_3Ge ⁶⁹	46	-	73
MgO/ Mn_2RuGa ⁷²	41	280	74
MgO/ $\text{Mn}_2\text{Ru}_{0.48}\text{Ga}$ ⁷²	54	221	21

Summary

- Cubic $\text{Mn}_2\text{Ru}_{-.5}\text{Ga}$ is the first example of the long-sought zero-moment half metal. It has 21 valence electrons
- Biaxially strained cubic films grow on MgO 001 at 350 °C
- They have perpendicular anisotropy ($K_u \sim 30 \text{ kJ m}^{-3}$) and huge coercivity.
- Curie temperature is ~ 200 °C
- Fermi-level spin polarization at room temperature is $\approx 60\%$
- The material creates no stray field, and it is immune to external field
- MRG may serve as the pinned layer in ultra-thin stacks with no SAF (read heads), but MTJs have to be built.
- It could serve as the storage layer in memory, but STT switching needs to be demonstrated.

XMCD 50 K



2. Playing with the polar catastrophe

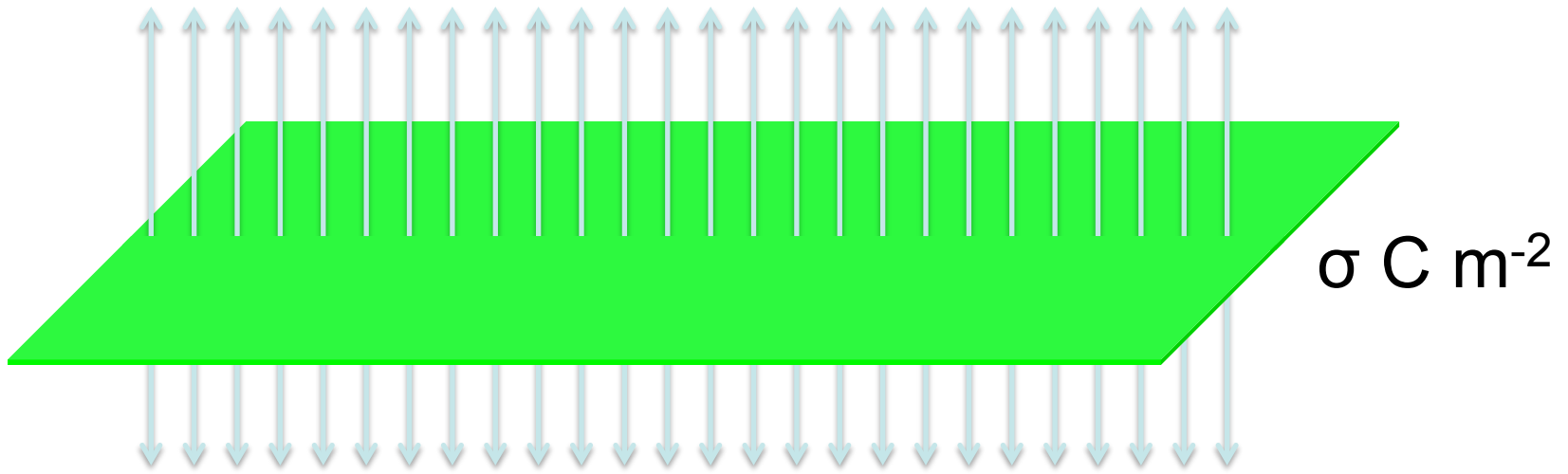
X. R Wang, W. M. Lv, Ariando, T. Venkatesan, H Hilgenkamp, J. M. D. Coey



H R Wang et al to be published

Zug 15-viii-2014

single charged sheet



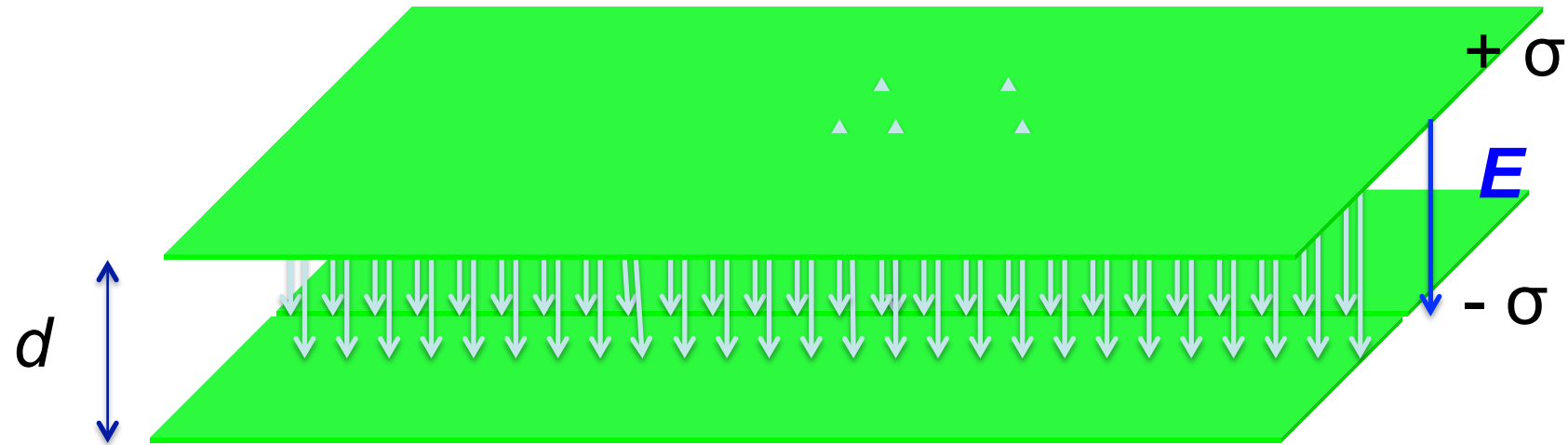
Gauss law: $\int E \cdot dA = q/\epsilon_0$ $\epsilon_0 = 8.854 \cdot 10^{-12} \text{ C V}^{-1}\text{m}^{-1}$

$$E = \sigma/2\epsilon_0 \quad \text{Taking } \sigma = 1 \text{ C m}^{-2}$$
$$E = 57 \cdot 10^9 \text{ V m}^{-1}$$

Energy density $\frac{1}{2}\epsilon_0 E^2 = \sigma^2/8\epsilon_0 = 14 \cdot 10^9 \text{ J m}^{-3}$
 $\rightarrow \infty!$

22 eV per unit cell! ($a_0 = 0.39 \text{ nm}$)

double sheet



$$E = \sigma/\epsilon_0 \quad \text{Taking } \sigma = 1 \text{ C m}^{-2}$$

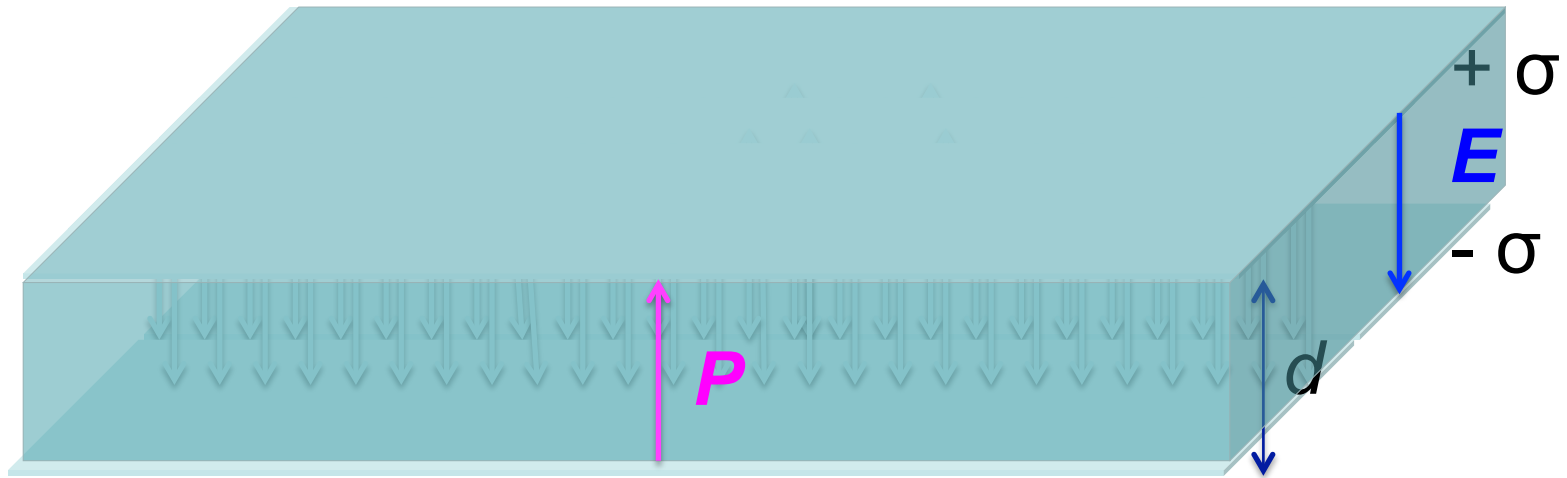
$$E = 113 \cdot 10^9 \text{ V m}^{-1}$$

$$\begin{aligned} \text{Areal energy density } (d/2)\epsilon_0 E^2 &= d\sigma^2/2\epsilon_0 \\ &= 22 \text{ J m}^{-2} \text{ if } d = a_0 \end{aligned}$$

$$\sim 20 \text{ eV}/a_0^2$$

Zug 15-viii-2014

ferroelectric slab



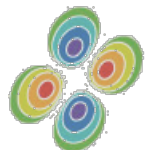
$$E = \sigma/\epsilon_0$$

$$P = -\epsilon_0 E = 1 \text{ C m}^{-2}$$

$$E = -\nabla V$$

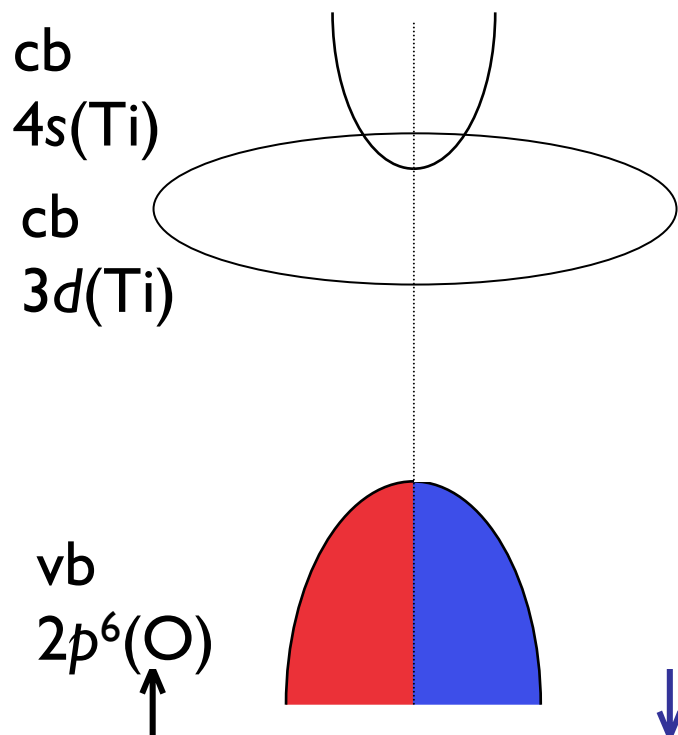
$$E = 113 \cdot 10^9 \text{ V m}^{-1}$$

The huge potential difference is neutralized by charges attracted to the free surfaces.

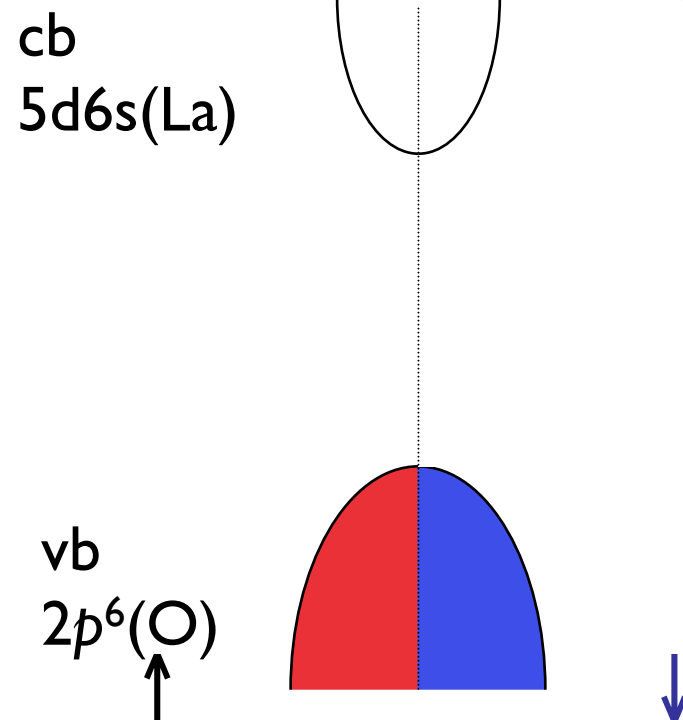


Perovskite interfaces

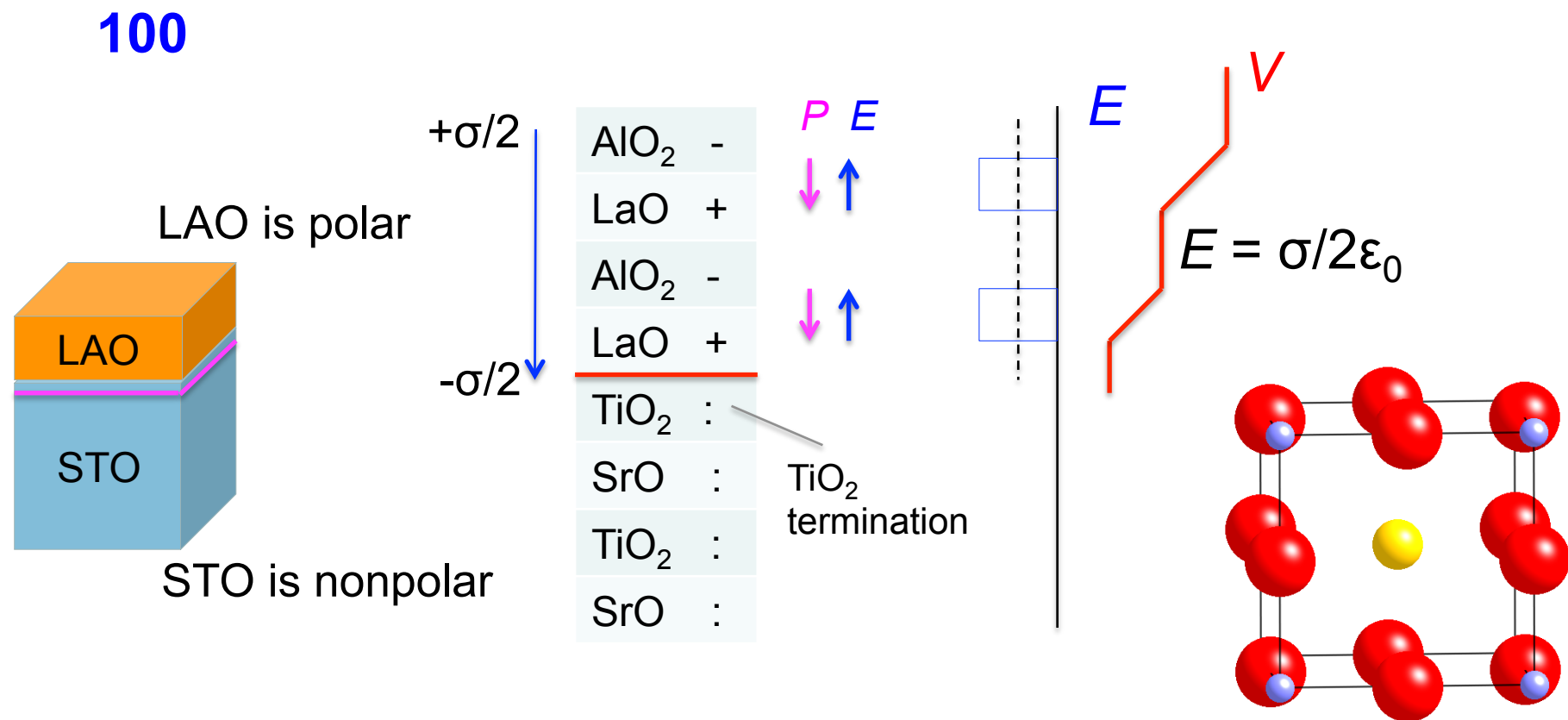
	E_g (eV)	a_0 (pm)	ϵ
SrTiO_3	3.2	391	300
LaAlO_3	5.6	379	24



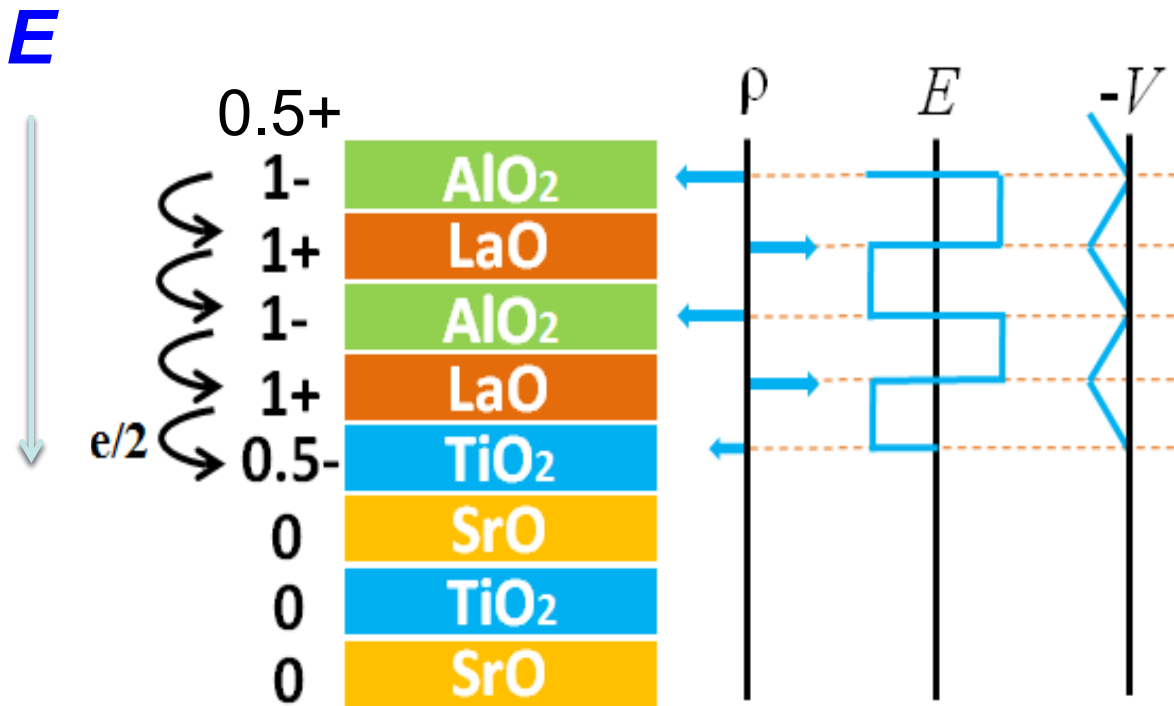
Zug 15-viii-2014



LaAlO_3



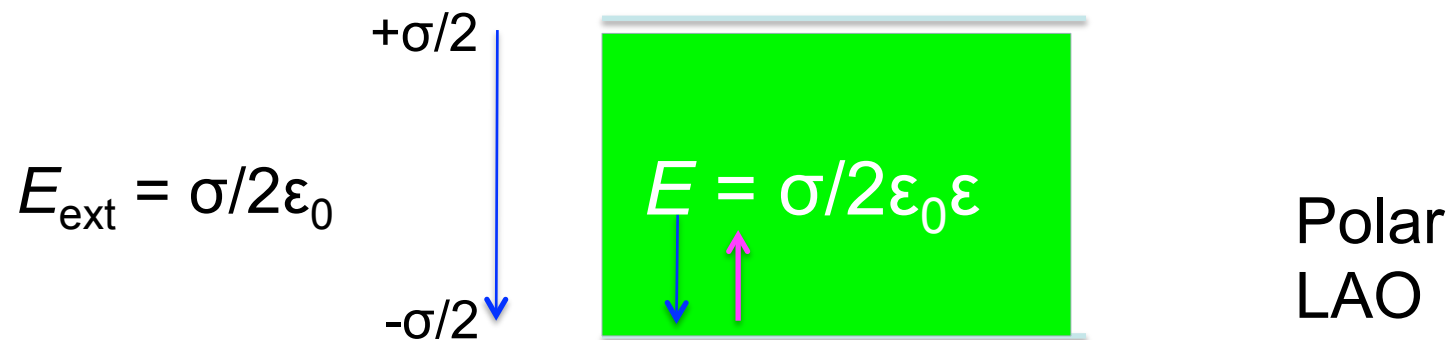
Charge transfer at the interface needed to avert the polar catastrophe is $0.5e / \text{uc}$, or $\sim 0.5 \text{ Cm}^{-2}$ or $3.3 \times 10^{18} \text{ electrons m}^{-2}$



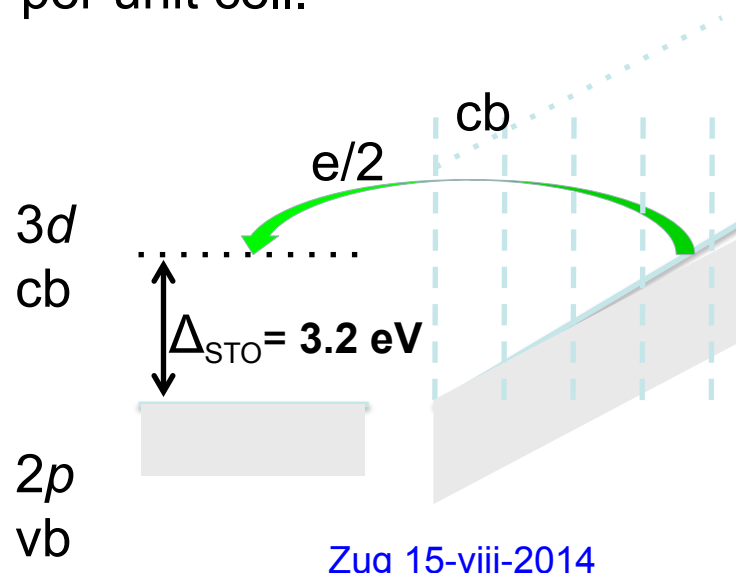
The surface charges of $\pm e/2$ create a field E that prevents the internal field from diverging.

The top and bottom interfaces of the polar oxide are coupled

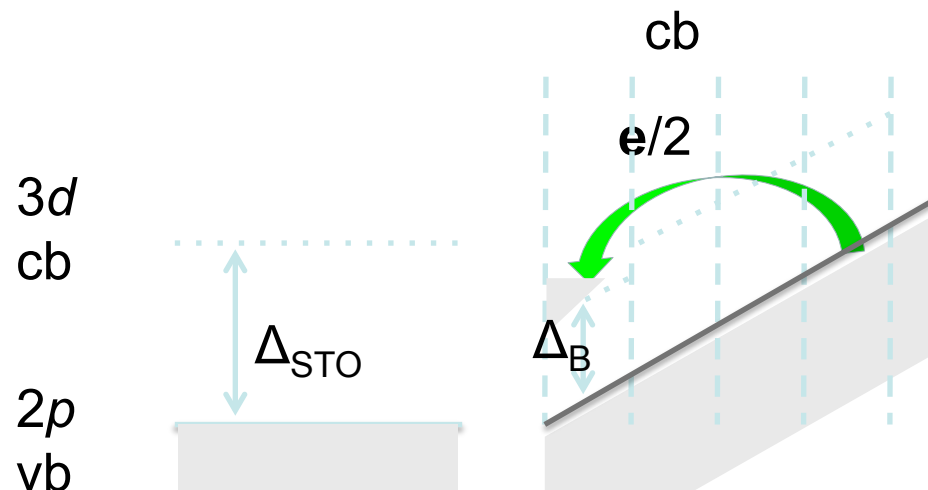
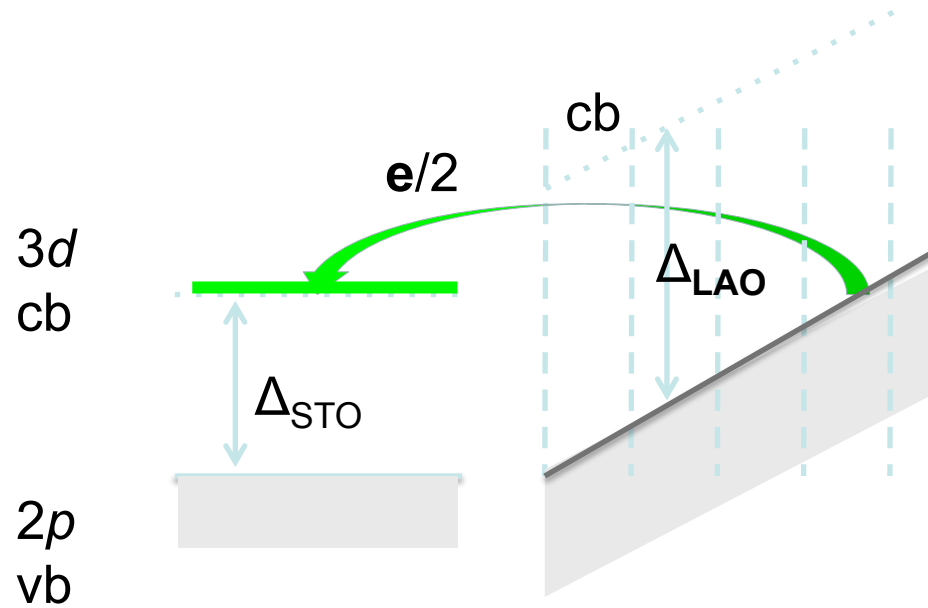
Where does the $-\sigma/2$ interface charge come from ?



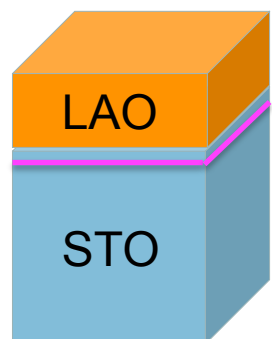
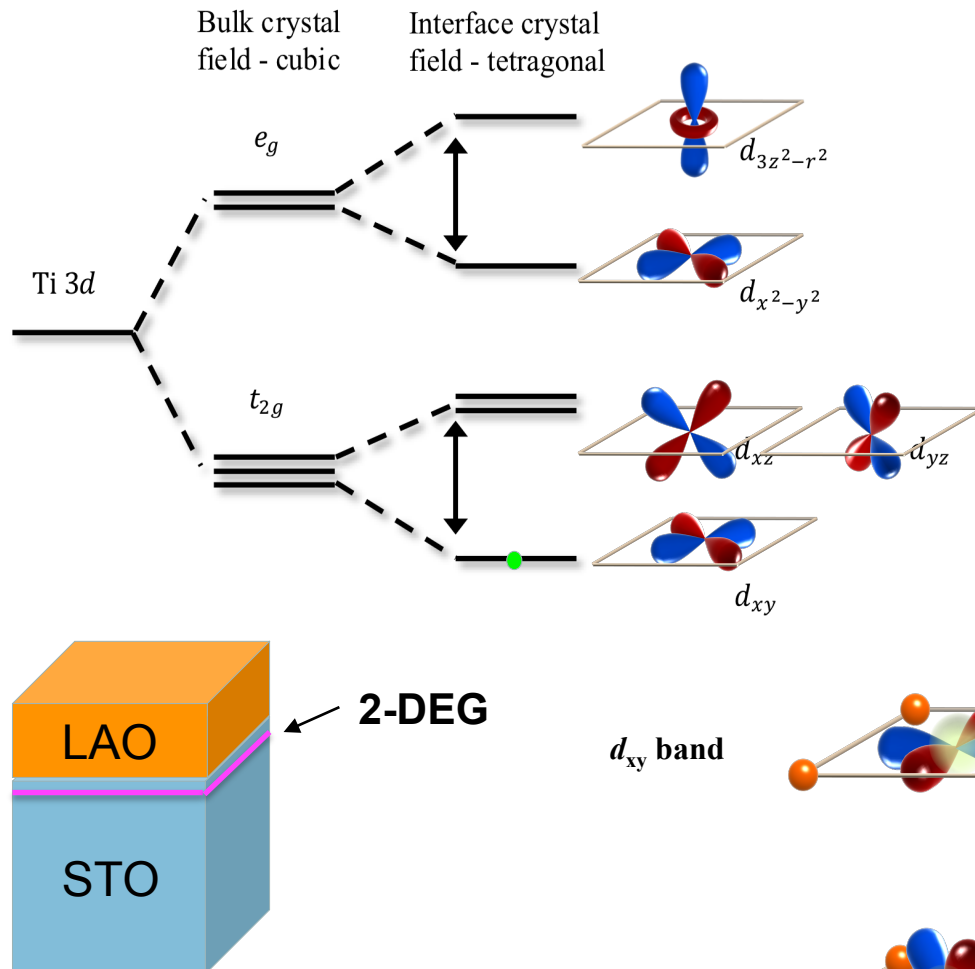
The internal field in LAO is reduced by a factor ϵ from 57 V nm^{-1} to 2.4 V nm or 0.9 V per unit cell.



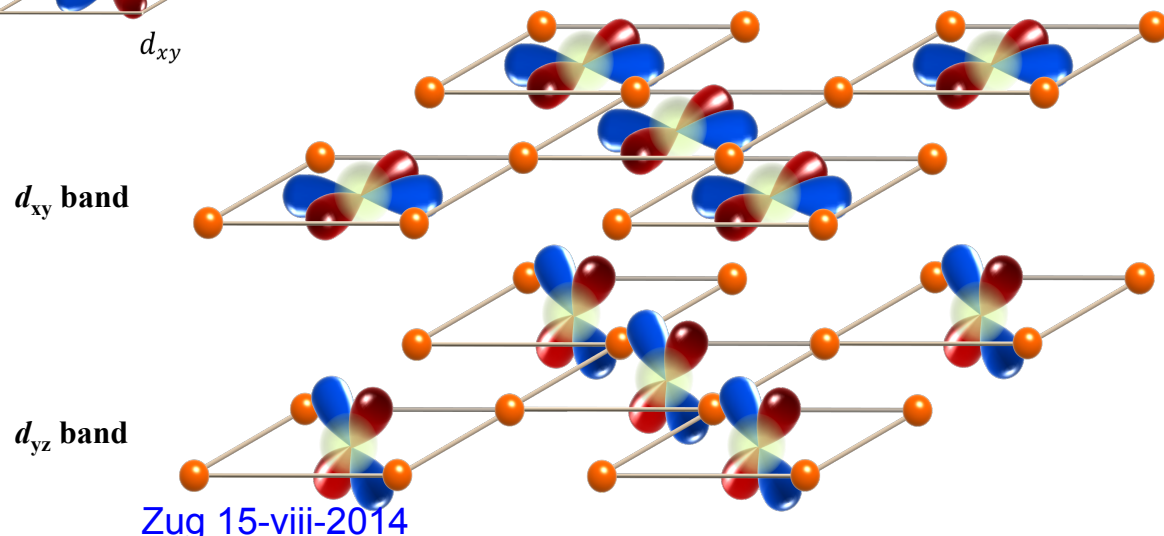
>4 uc of LAO are needed for electrons to be transferred to the bottom of the $3d(\text{Ti})$ band.



The 2-DEG at the STO interface is ferromagnetic



- Intrinsic or defect-induced ?
- d_{xy} or $d_{yz/zx}$ (or $d_{x^2-y^2}$)
- Uniform or inhomogeneous?
- T_C ?



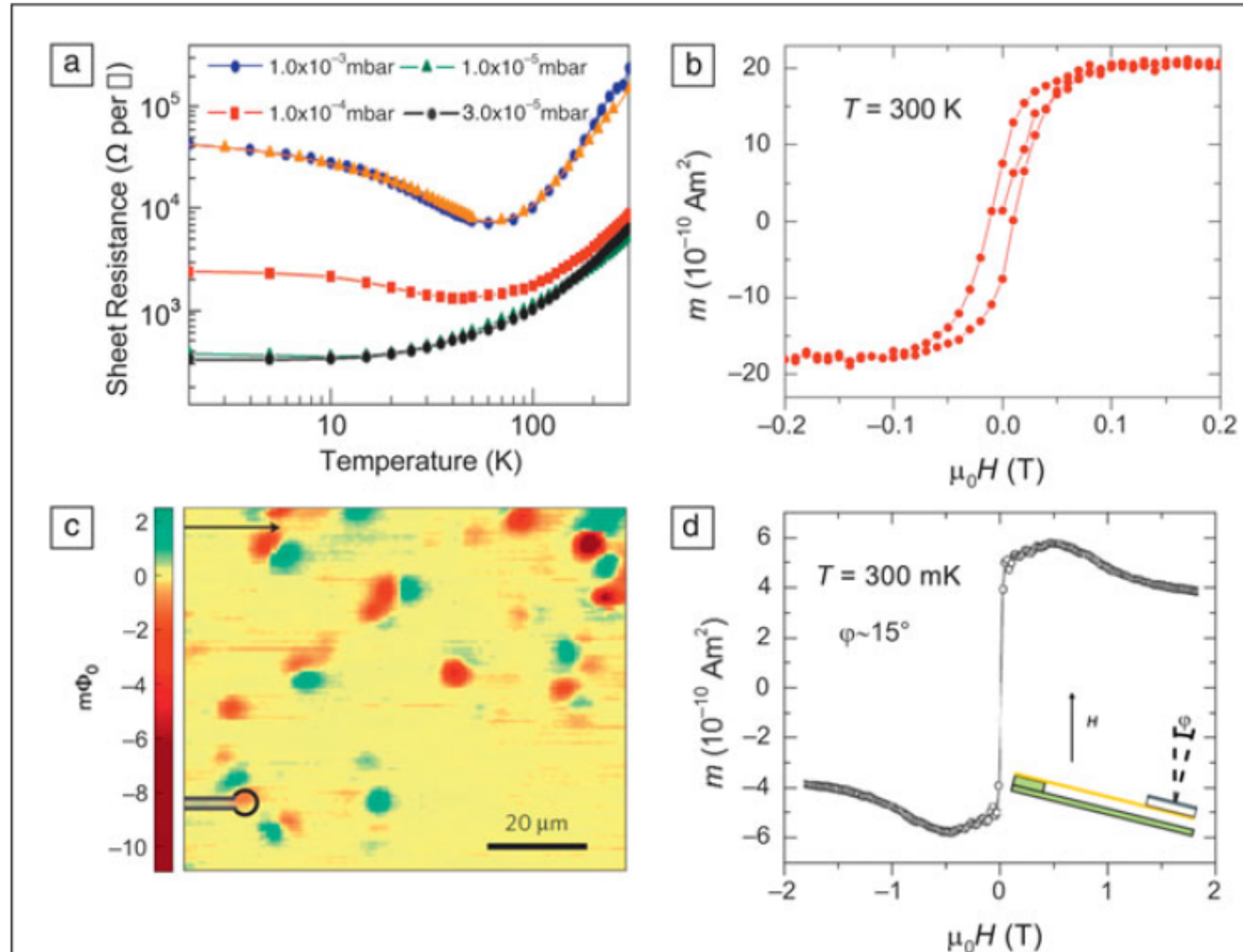
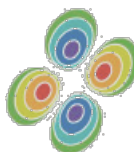
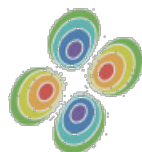
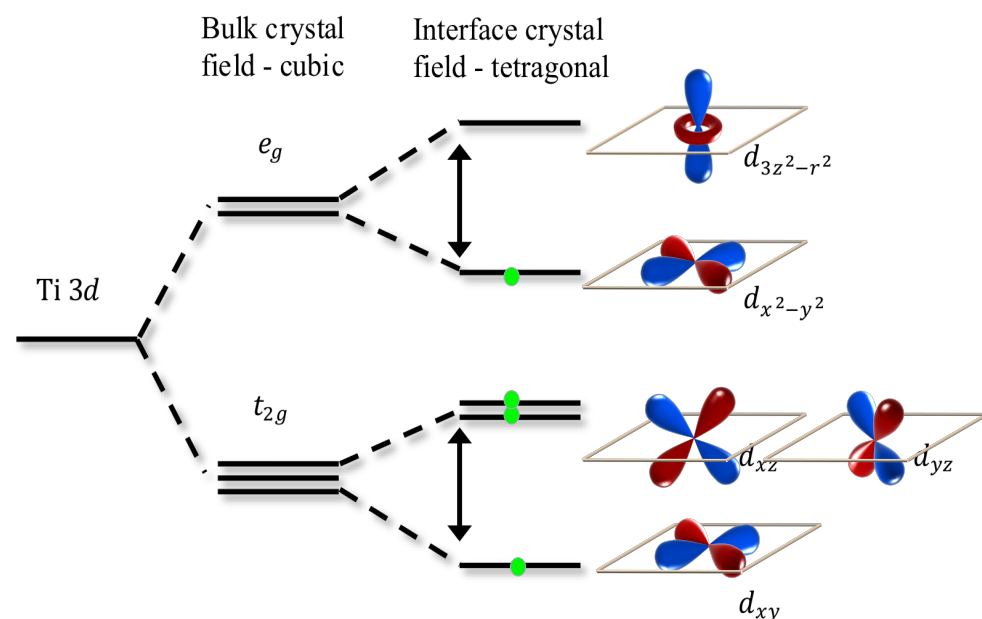
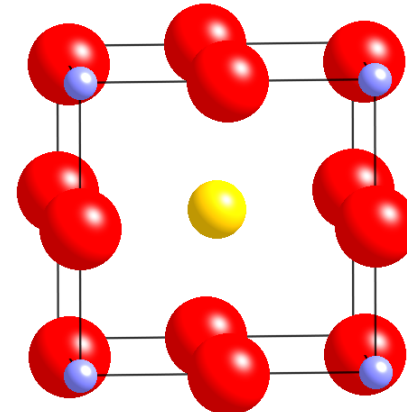


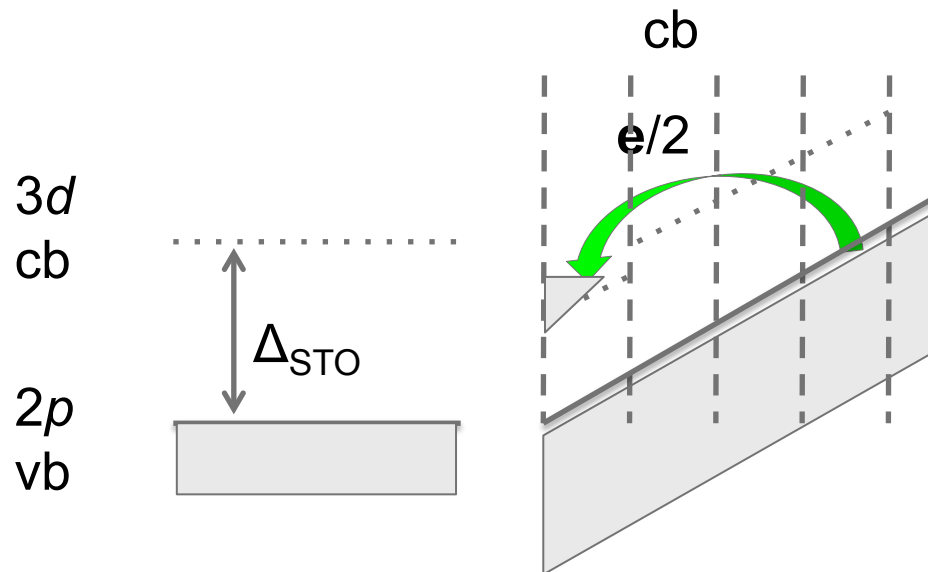
Figure 5. Evidence for magnetism of the two-dimensional electron gas at the $\text{LaAlO}_3/\text{SrTiO}_3$ interface. (a) Resistance showing a minimum associated with Kondo scattering for samples deposited at various oxygen pressures. Figure adapted with permission from Reference 51. (b) Magnetic moment measured with SQUID-VSM. Figure adapted with permission from Reference 52. (c) Direct imaging of a magnetic stray field using a scanning SQUID microscope. Figure adapted with permission from Reference 7. (d) Moment detected by torque magnetometry. Figure adapted with permission from Reference 54.

LaMnO₃

Orthorhombically-distorted perovskite $\sqrt{2}a_0, \sqrt{2}a_0, 2a_0$

Mn³⁺ 3d⁴ ($t_{2g}^3 e_g^1$) is a Jahn-Teller ion that deforms its cubic environment. The oxide is an insulator, with in-plane orbital order and A-type antiferromagnetic order. $T_N = 115$ K.
Thin films are often ferromagnetic





In LaMnO_3 , $\epsilon = 70$, $E_0 = 0.85 \text{ Vnm}^{-1}$, $\Delta = 1.3 \text{ eV}$
 $\Delta/E_0 = 4 \text{ uc.}$

The charge transfer occurs within the manganite layer.

The extra electrons in the $3d$ band create some $\text{Mn}^{2+} 3d^5$ states, and electron hopping introduces additional interlayer ferromagnetic exchange.

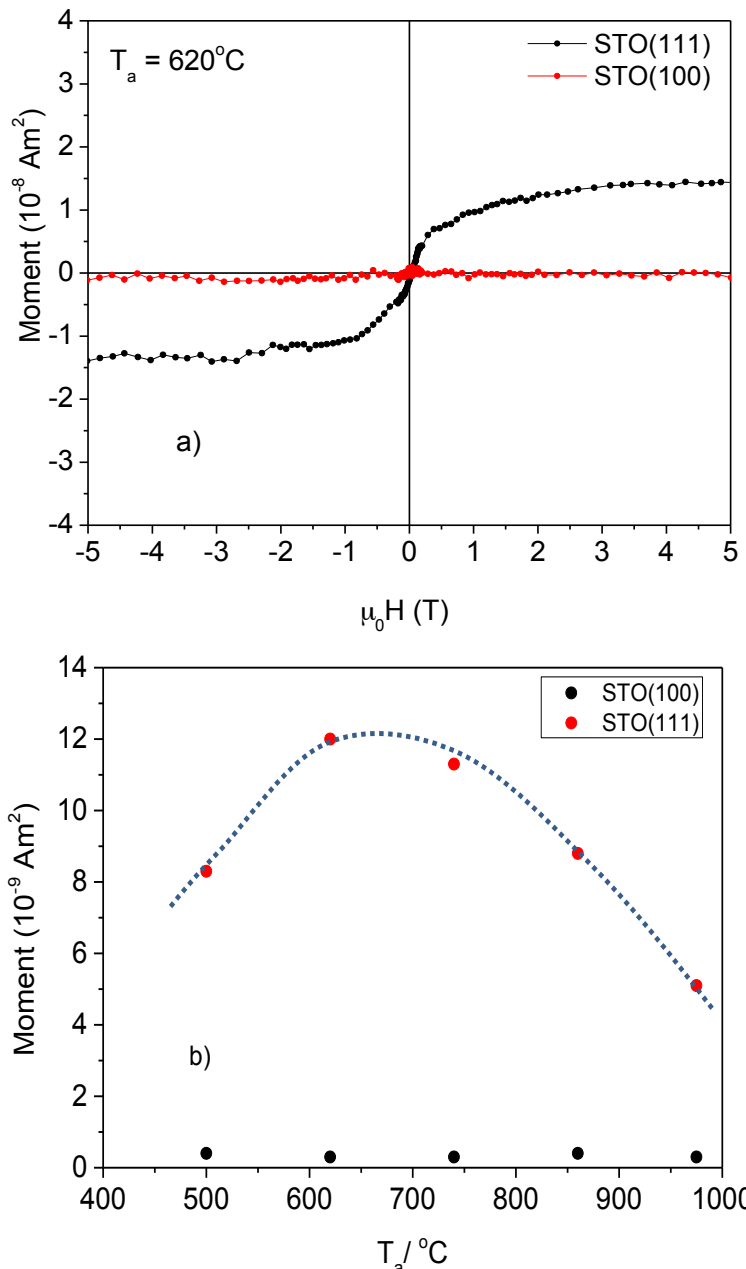
3. d^0 Magnetism

K.Ackland, M.Venkatesan, P.Stamenov, S.Sen J. M. D. Coey

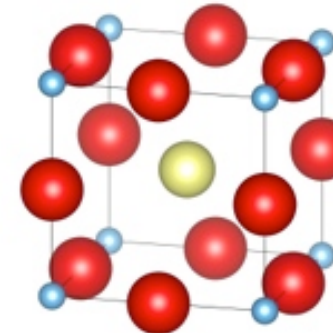


J. M. D. Coey et al, New J Phys 12, 053025 (2010).

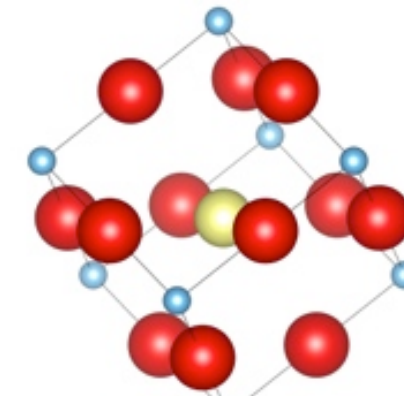
Zug 15-viii-2014



SrTiO₃



100



111



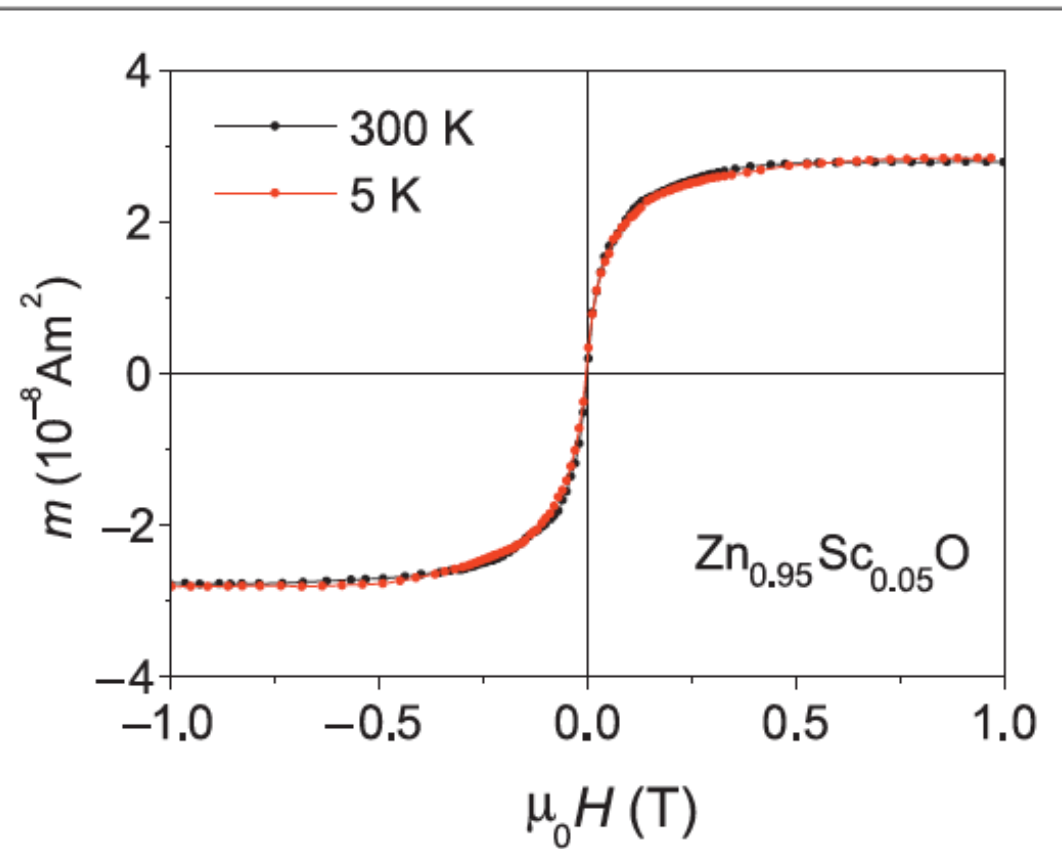
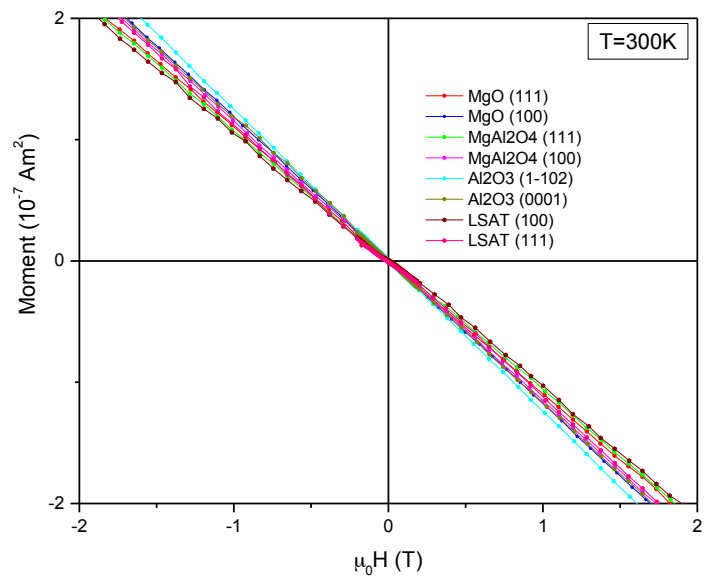
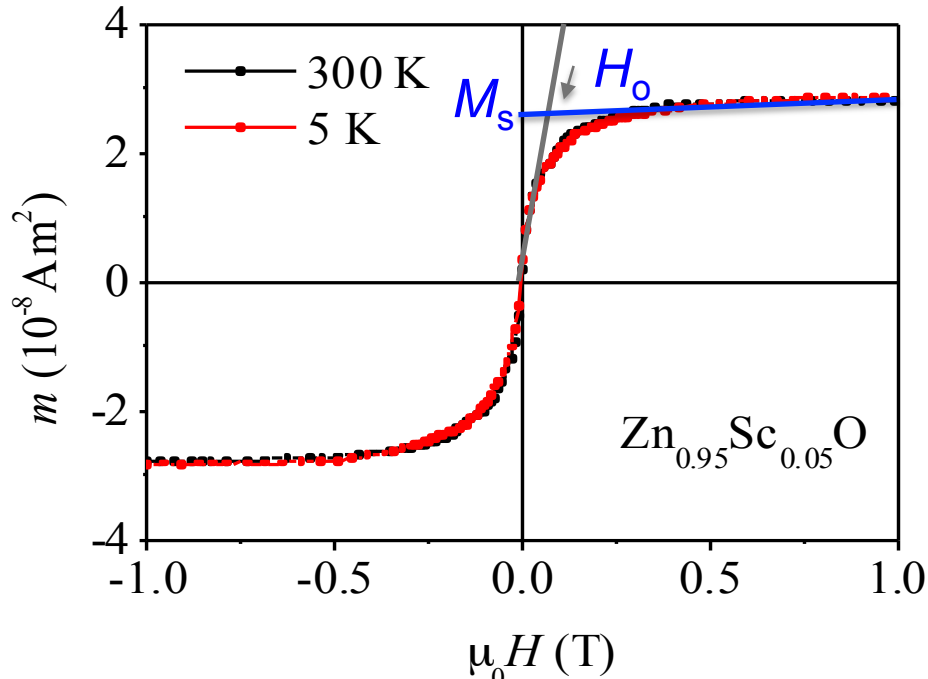


Figure 4. Magnetization of a typical d^0 material, a thin film of zinc oxide doped with scandium. The magnetization curves measured at temperatures between 4 K and 300 K exhibit a ferromagnetic-like saturation, with magnetization curves that superpose, after correction for the high-field slope. Figure adapted with permission from Reference 66.

d^0 magnetism

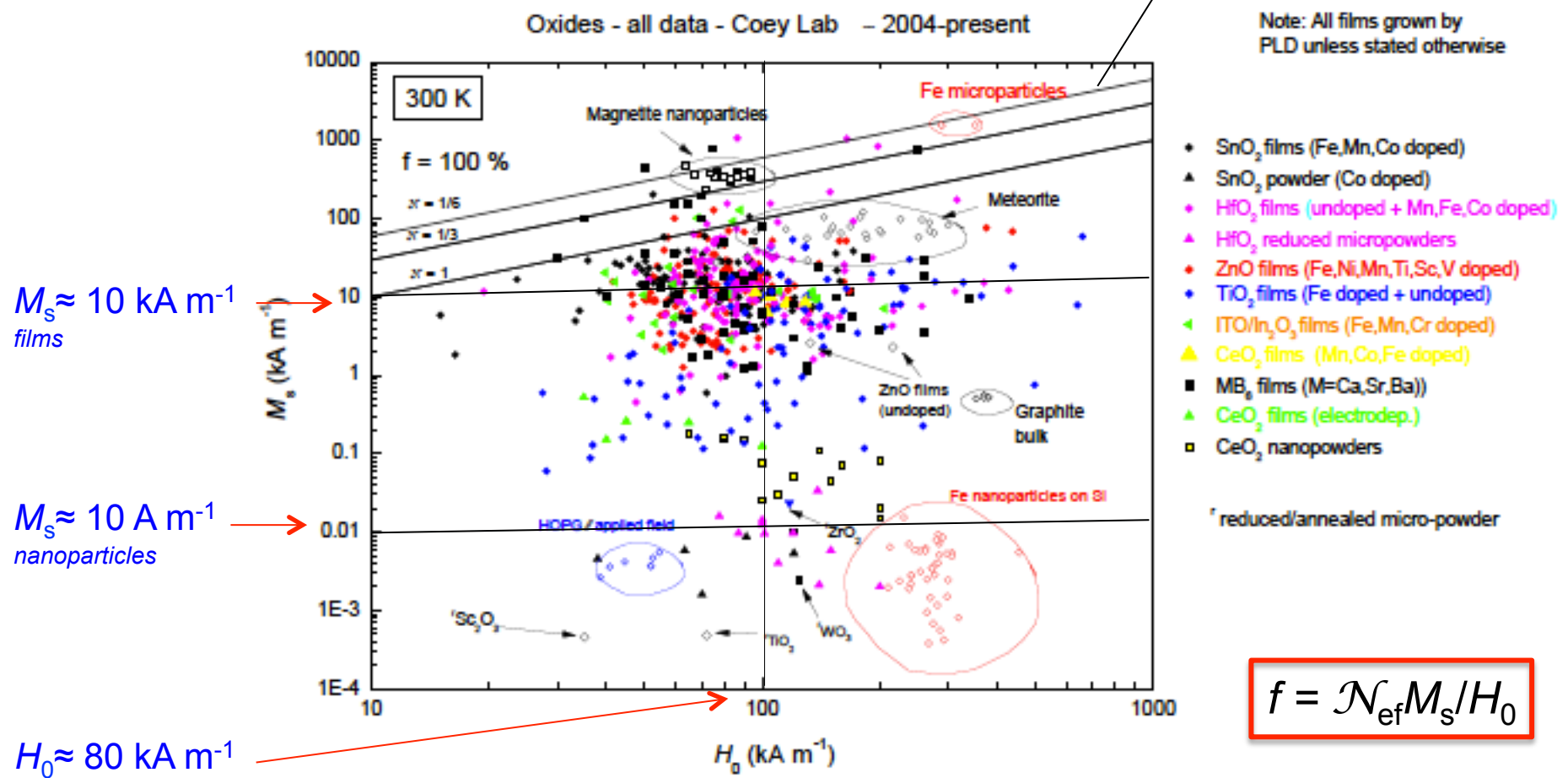


- Found for doped and undoped oxide thin films and nanoparticles
- At first they were thought to be ferromagnetic dilute magnetic semiconductors (DMS) $\text{Zn}_{0.95}\text{Co}_{0.05}\text{O}$
- 3d dopants do not order magnetically
- Magnetism is defect-related and *poorly-reproducible*

- Independent of temperature $\rightarrow T_C >> RT$
- anhysteretic \rightarrow dipole interactions
- $M_s \ll H_0$ \rightarrow A tiny volume fraction f is ferromagnetic

All Oxide data

100% volume fraction



We need a ‘fruitfly’ system, where the data is reproducible, and no extraneous explanation is possible



CeO₂ nanoparticles - Literature

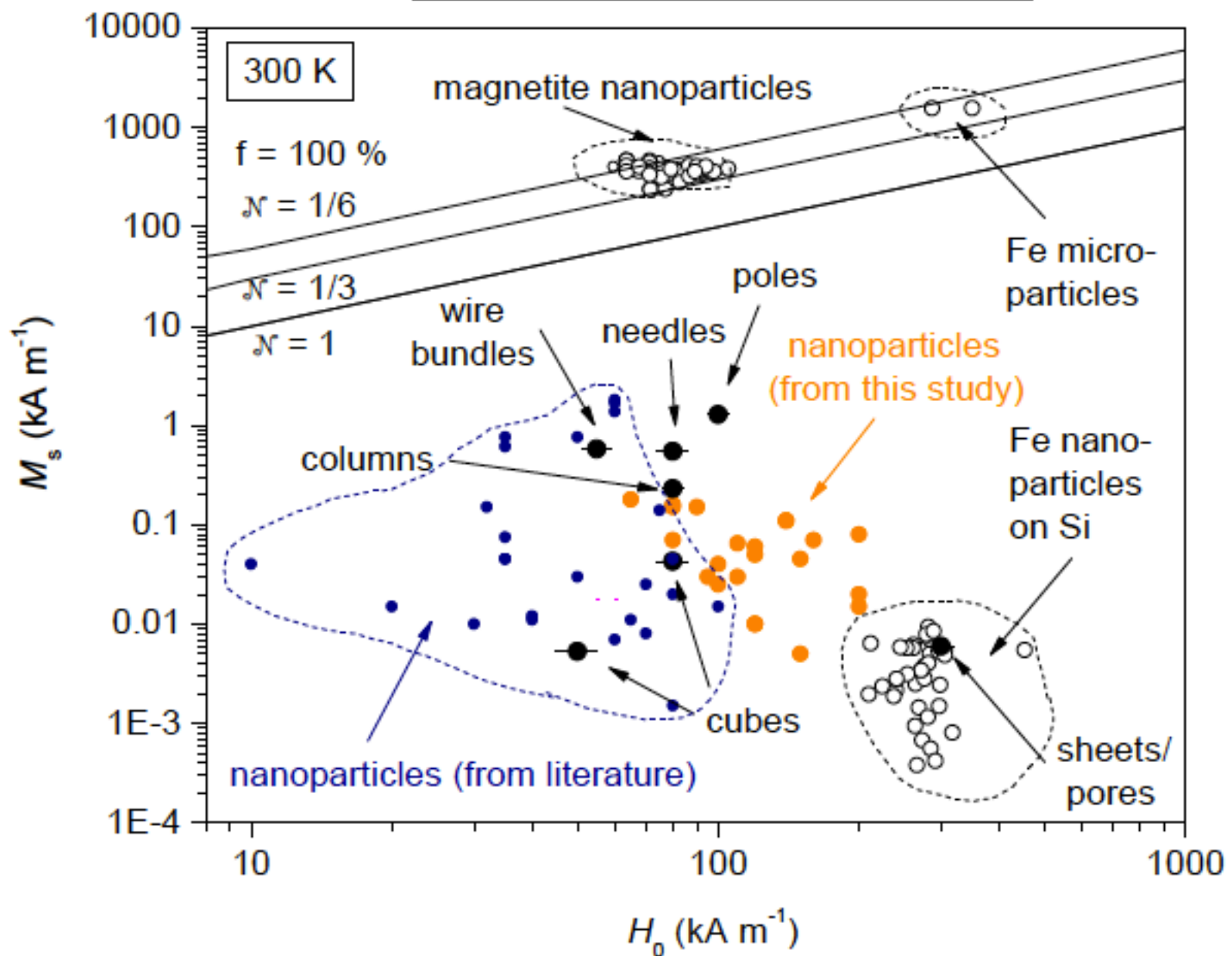
Literature data on magnetization, extrapolated saturation field H_0 and magnetic volume fraction f for CeO₂ nanoparticles

Av. radius r_0 (nm)	M_s (Am ⁻¹)	H_0 (kAm ⁻¹)	f^* (10 ⁻⁶)	Surface treatment
3.5	7	60	40	-
7.5	11	40	90	-
5×1	550	80	2300	PEG
3	40	80	160	Oleic acid
3.5	1.5	120	4	Glutamic acid
2.7	25	70	120	NH ₄ OH
1.8	760	50	500	1,2 dodecandiol
2.5	150	32	1500	PEG
4.6	120	110	360	PVP
3.0	140	90	520	-
2.0	84(46)	120(38)	233	PEG

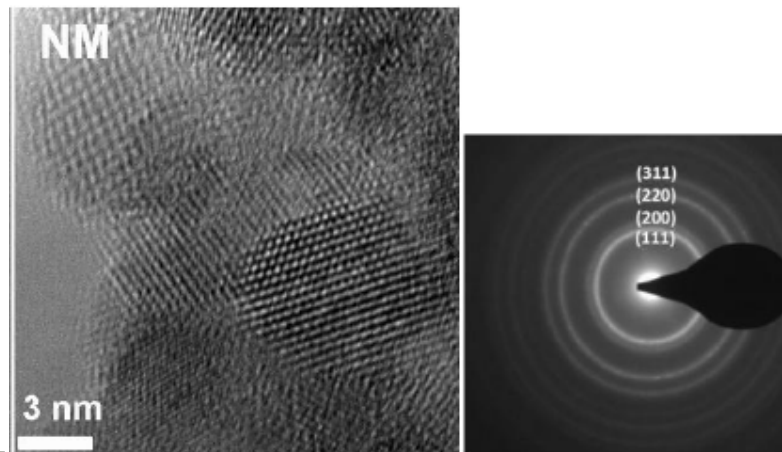
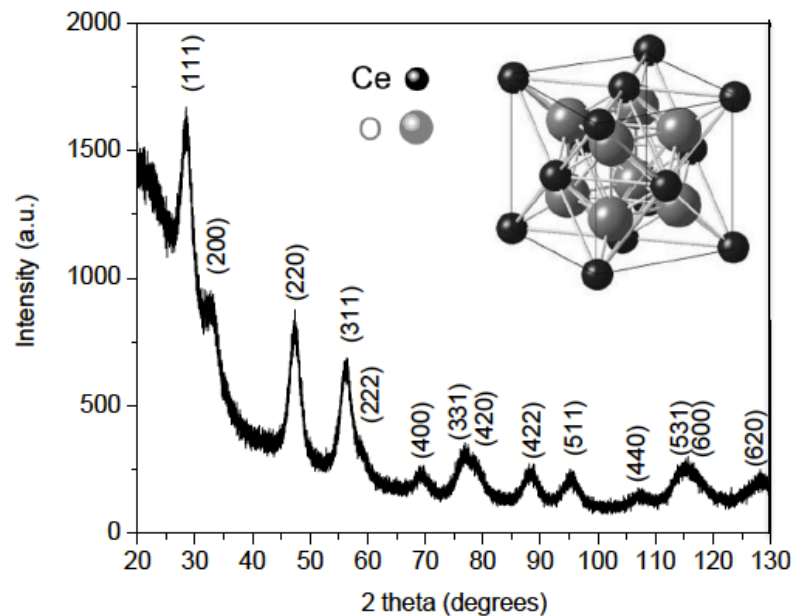
- $$f = \mathcal{N}_{\text{eff}} M_s / H_0$$

$$\mathcal{N} \approx 1/3$$

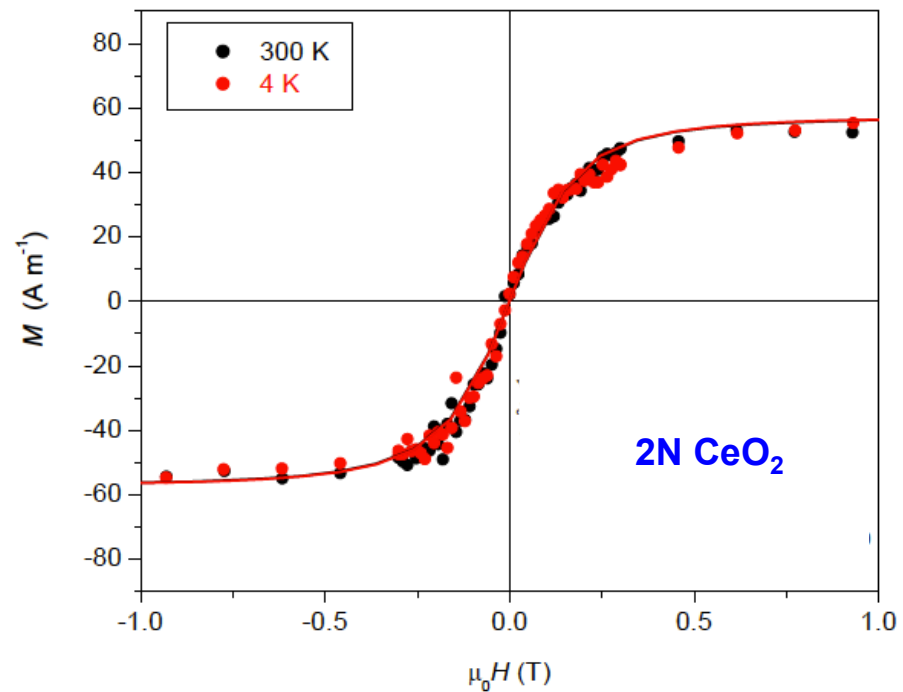
Undoped CeO₂ nanostructures



CeO₂ nanoparticles - Characterization

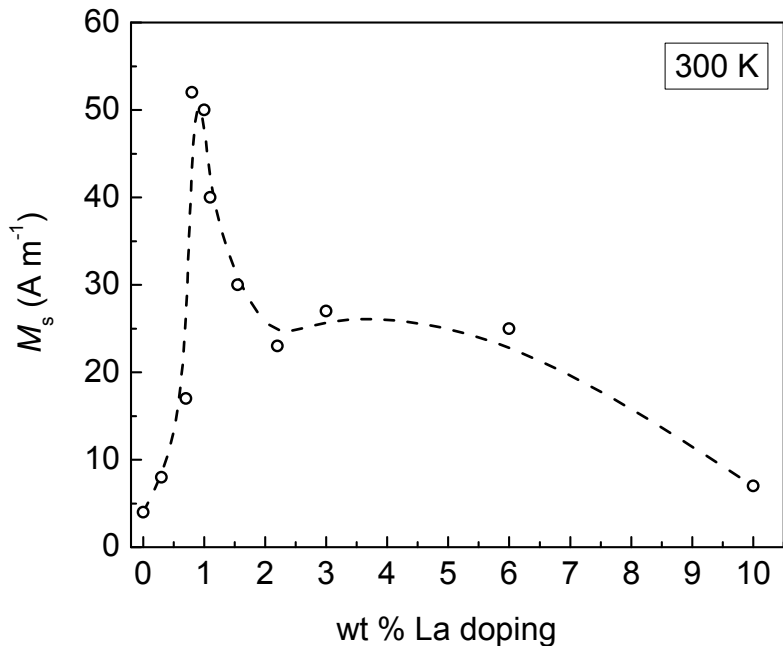


SPIN ELECTRONICS
TRINITY COLLEGE, DUBLIN

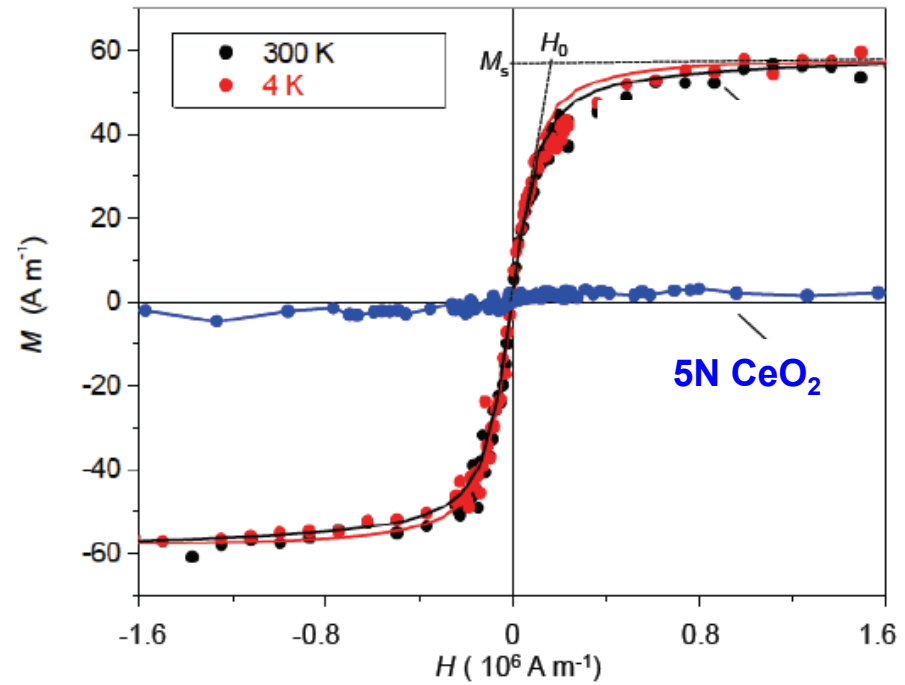


Uniform 4 nm CaF₂-structure nano particles of CeO_{2-δ} are precipitated from CeNO₃ + PEG solution. Moment $\sim 0.2\mu_B/\text{particle}$ (900 Ce)

CeO₂ nanoparticles – La doping



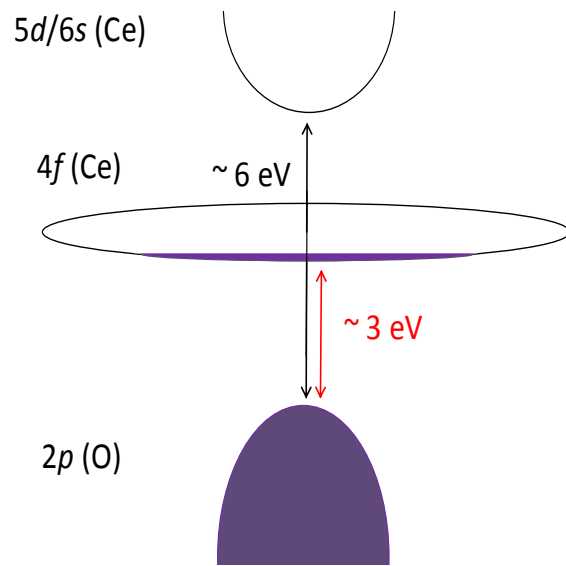
La-doping of 5N pure CeO_{2- δ} turns on the moment — maximum for 1%



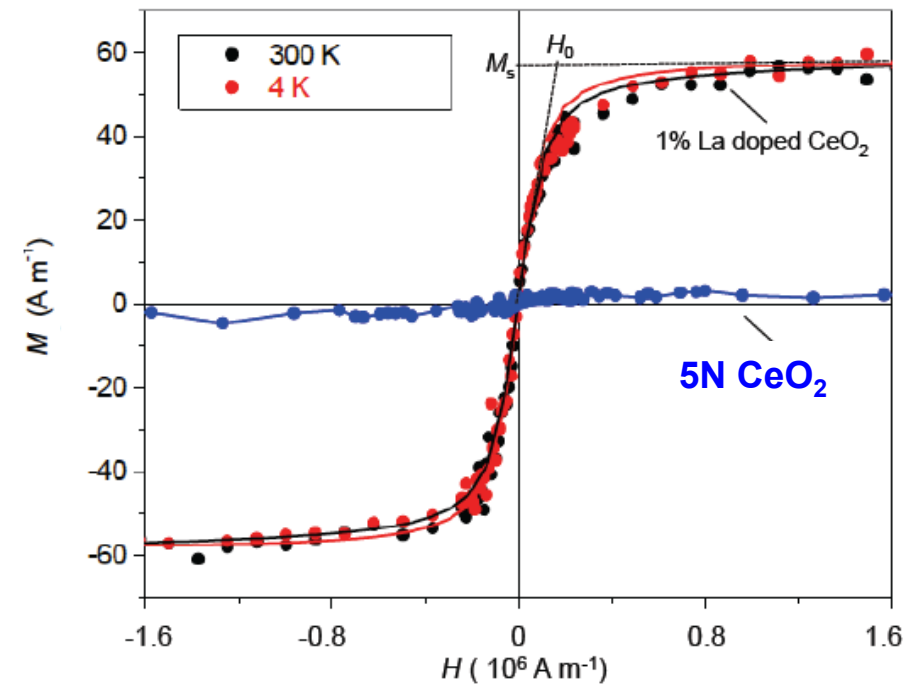
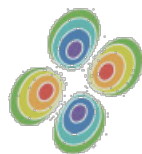
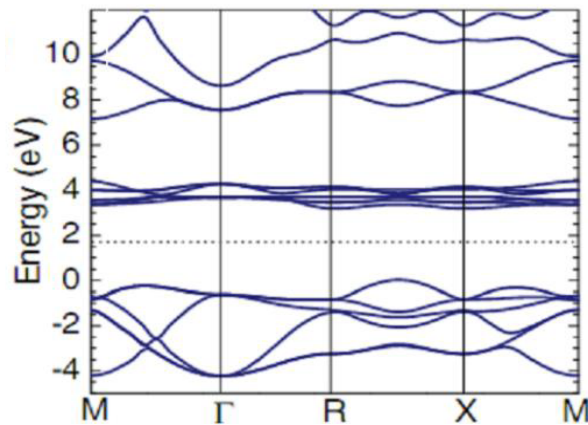
Nanoparticles from 5N precursor are not magnetic, but 2N particles showed ‘ferromagnetic’ signal.

$\Sigma 3d$ impurities < 10 ppm.

CeO₂ nanoparticles



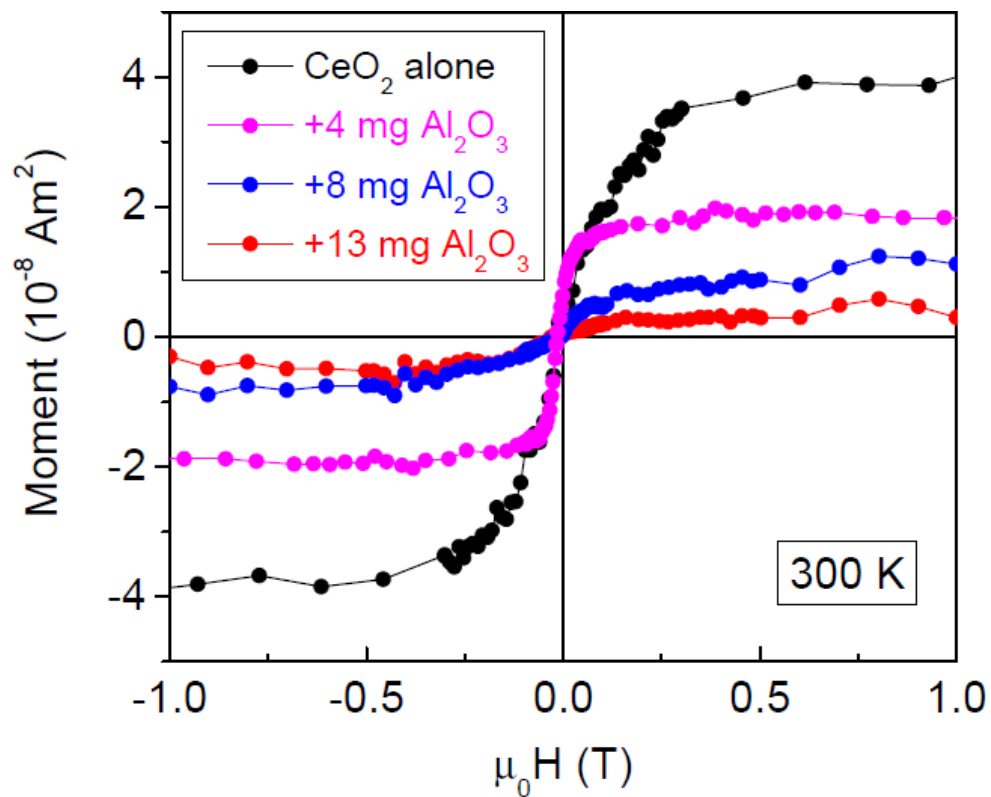
Any Ce 4f electrons are delocalized (~ no Curie-law upturn in susceptibility < 0.4% of Ce).



Nanoparticles from 5N precursor are not magnetic, but 2N particles showed ‘ferromagnetic’ signal, due to La impurities

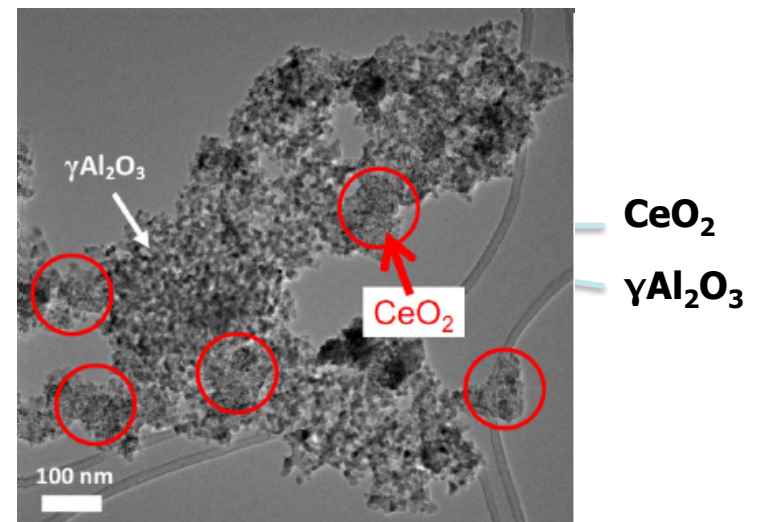
Surfaces of oxygen-deficient nanoparticles are conducting

Effect of dilution– 15nm $\gamma\text{Al}_2\text{O}_3$



Progressive dilution with nonmagnetic 15nm $\gamma\text{Al}_2\text{O}_3$ nanoparticles **makes the moment disappear!**

6 x dilution (by volume) reduces moment by 94%

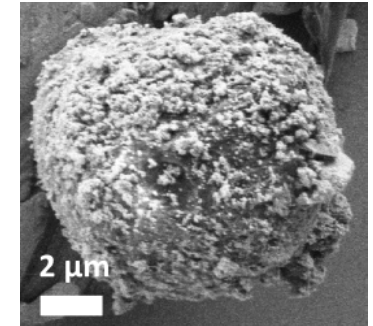
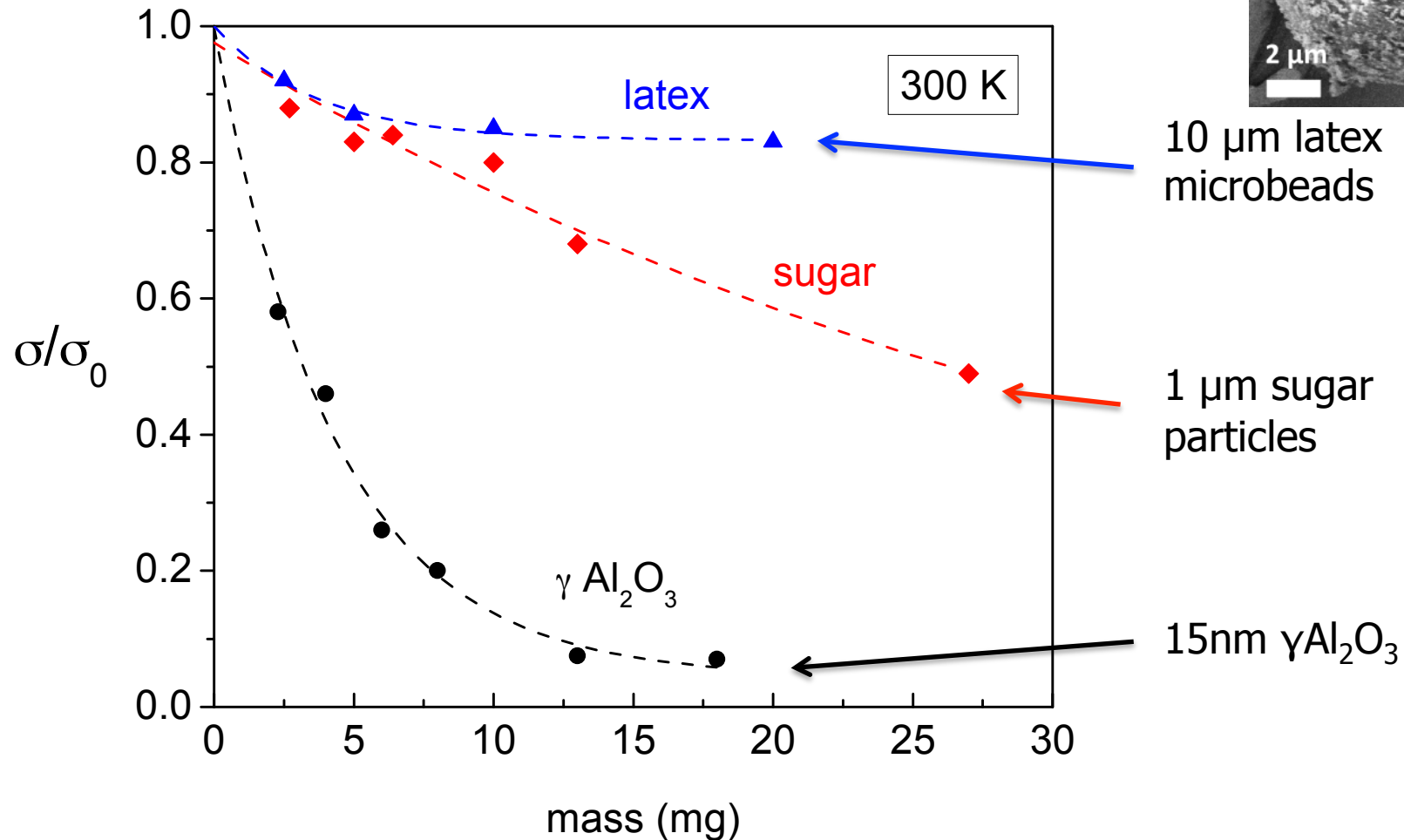


Dilution with 15nm $\gamma\text{Al}_2\text{O}_3$ breaks the CeO_2 into clumps < 100 nm in size

Moment is *stable* in time. It diminishes by < 10% in a year



Dilution – Summary



10 μm latex
microbeads

1 μm sugar
particles

15nm $\gamma\text{Al}_2\text{O}_3$

The smallest particles are most effective.

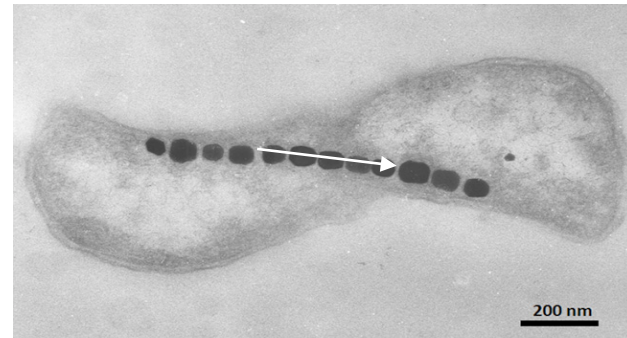
After dissolving the sugar, the moment reappears (increased)

Zug 15-viii-2014

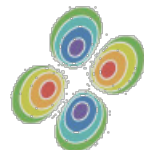
Summary of results

This behavior seems unprecedented in the literature on magnetism:
There is no evidence of superparamagnetism (scaling of M with H/T) and
 H_{dipolar} is 1000 times too small for superferromagnetism

1. The **energy scale** is unusually large. The absence of temperature dependence from 4 K to 300 K suggests a 'Curie temperature' of order 1000 K
2. There is a mesoscopic **length scale** of order 100 nm needed for a collective magnetic response to appear.



➤ How can we understand it ?

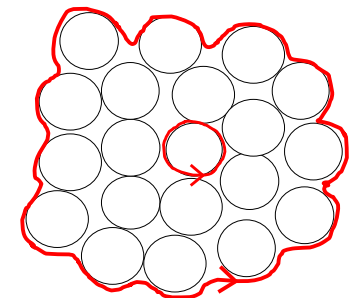


An explanation

- It has nothing to do with ferromagnetism (No Ce compound has $T_c > 125$ K!)

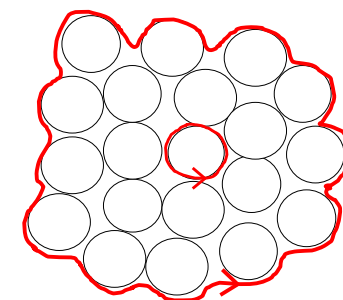
An explanation

- It has nothing to do with ferromagnetism (No Ce compound has $T_c > 125$ K!)
- We are looking at **giant orbital paramagnetism** associated with persistent electric currents **in coherent domains** > 100 nm is size.



An explanation

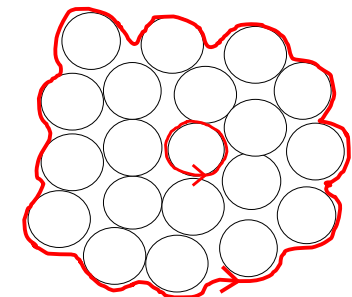
- It has nothing to do with ferromagnetism (No Ce compound has $T_c > 15$ K!)
- We are looking at **giant orbital paramagnetism** associated with persistent electric currents **in coherent domains** > 100 nm is size.



- Quantum field theory envisages such coherent domains due to resonance with vacuum fluctuations of the electromagnetic field. (cf Casimir force), which renormalizes the interaction by \sqrt{N} , where N is the number of particles (Ce atoms) in the coherent domain .

An explanation

- It has nothing to do with ferromagnetism (No Ce compound has $T_c > 15$ K!)
- We are looking at **giant orbital paramagnetism** associated with persistent electric currents **in coherent domains** > 100 nm is size.



- Quantum field theory envisages such coherent domains due to resonance with vacuum fluctuations of the electromagnetic field. (cf Casimir force), which renormalizes the interaction by \sqrt{N} , where N is the number of particles (Ce atoms) in the coherent domain.
- The theory predicts that the magnetization curve should be of the form

$$M = M_s x / (1 + x)^{1/2} \quad (1)$$

An explanation

$$\mathcal{H} = \sum_{i=1}^N L_i^2 / 2mr^2 + \mathbf{A} \cdot \mathbf{J}$$

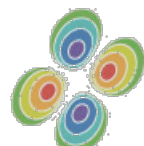
$$P = \mathbf{e}_\mu \cdot \mathbf{e}_B,$$

$$P = \kappa \sin 2\alpha \quad \kappa \approx 0.37$$

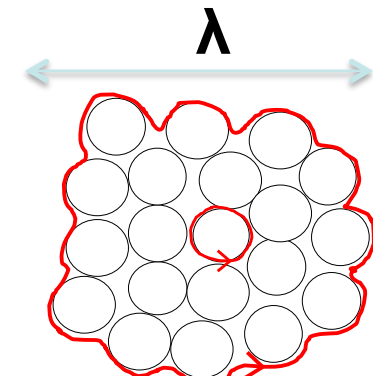
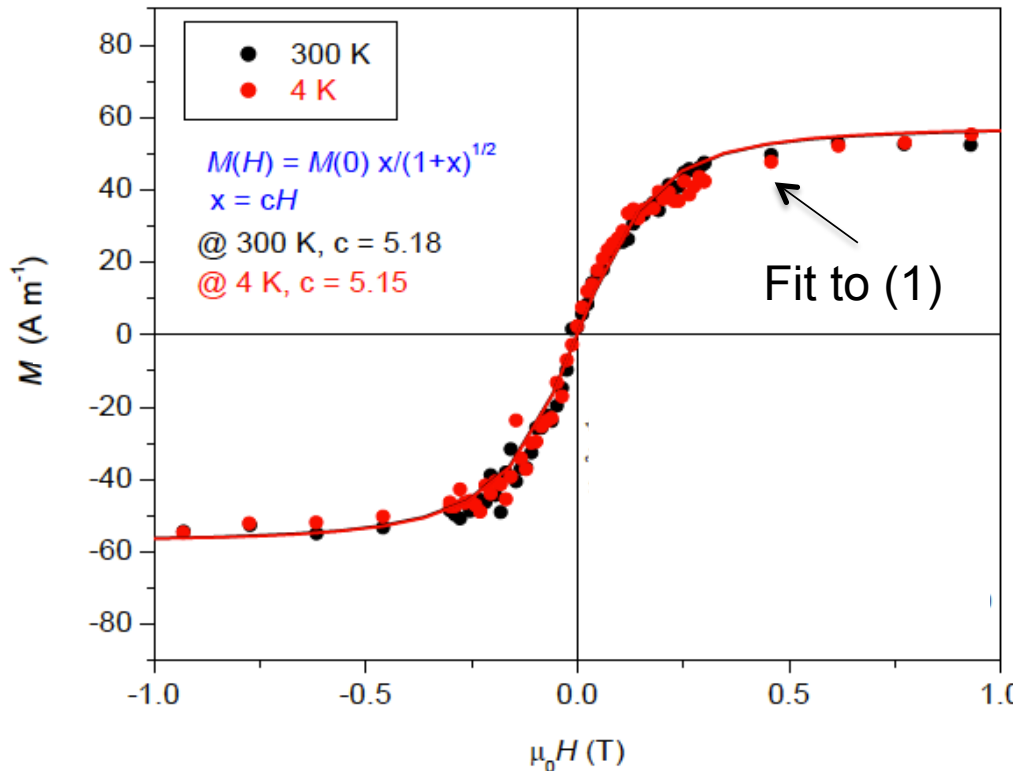
$$\tan \alpha = [1 + (1+x^2)^{1/2}] / x,$$

$$x = 2V/\hbar\omega = cB \quad V = \mu B$$

$$P = \kappa x / (1 + x^2)^{1/2} \quad (1)$$



An explanation



$$x = CB \quad (2)$$

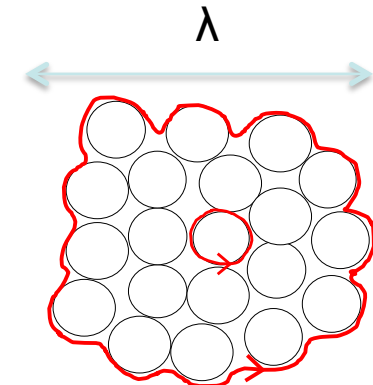
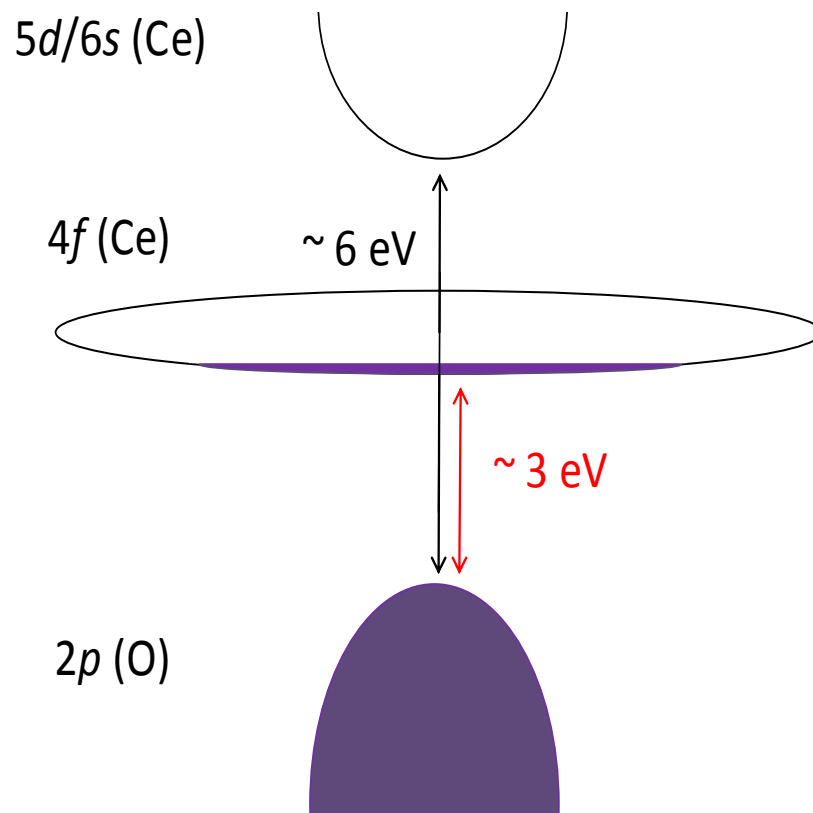
$$\begin{aligned} x &= 2V/\hbar\omega \text{ where } V = mB \\ &= (\pi/6)\lambda^3 MB \end{aligned}$$

$\lambda = 2\pi c/\omega$ the wavelength of the em radiation is identified with the size of the coherent domain

$$\boxed{\lambda^4 = 3hcC/\pi M_s} \quad (3)$$

- Fitting the magnetization curves gives both the **length scale** and the **energy scale** for the system

An explanation



$$C = 9.4 (7) \text{ T}^{-1}$$

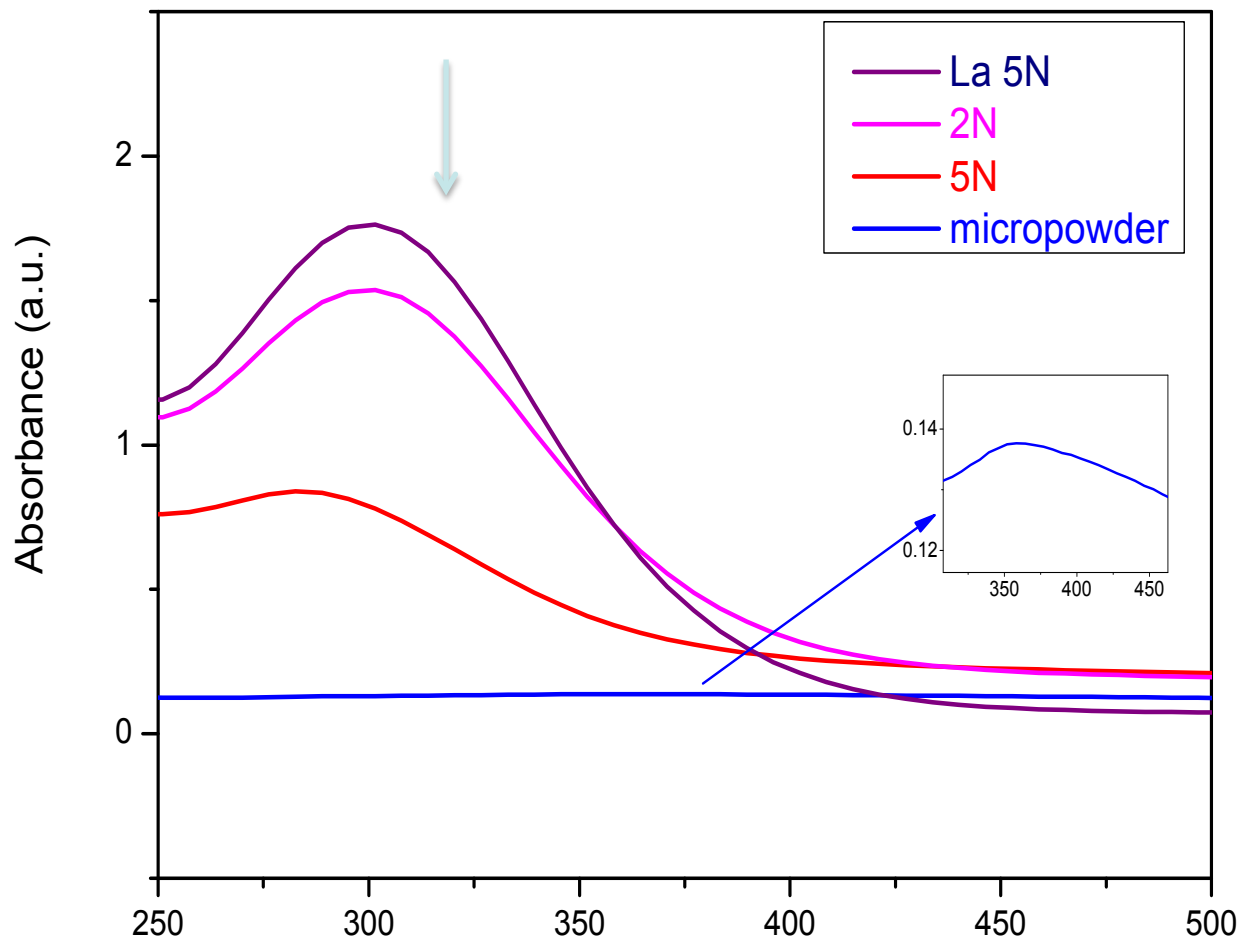
$$M = 58 \text{ Am}^{-1}$$

$$\lambda = 327 \text{ nm}$$

$$\hbar\omega = 3.8 \text{ eV}$$

A coherent domain is 320 nm in size contains $N = 5 \cdot 10^8$ Ce atoms or $\sim 5 \cdot 10^5$ nanoparticles with a moment $\mu = 2 \cdot 10^5 \mu_B$. The moment per nanoparticles in the coherent domain is $2.4 \mu_B \rightarrow 8\%$ of the sample is in the coherent state.

UV absorption spectrum



Summary

- Clusters of 4 nm CeO₂ nanoparticles exhibit *giant orbital paramagnetism*.
- The orbital currents are due to resonant coupling with zero-point fluctuations of the electromagnetic field in coherent domains ~ 300 nm is size.
- This *may* be the first evidence of an influence of these fluctuations in condensed matter.
- If true, many more manifestations of the effect are anticipated (Water at biological membranes, interfacial nanobubbles.....)

Conclusions

- Magnetism at the edge is full of shocks and surprises
- Biaxial strain on an oxide substrate has enabled growth of Cubic $\text{Mn}_2\text{Ru}_{0.5}\text{Ga}$ is the first zero-moment half-metal. Its usefulness in spin electronics now has to be demonstrated.
- Large orbital moments may be lurking near the surface of (some) 3d ferromagnetic films.
- The 2-dimensional electron gas forming in 100 SrTiO_3 near an interface with 100 LaAlO_3 to avert a polar catastrophe is ferromagnetic.
- The same mechanism switches thin films of LaMnO_3 from antiferromagnetic to ferromagnetic
- d^0 magnetism cannot be explained within the existing paradigm
- $m_{\text{sample on substrate}} \neq m_{\text{sample}} + m_{\text{substrate}}$

2014



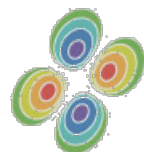
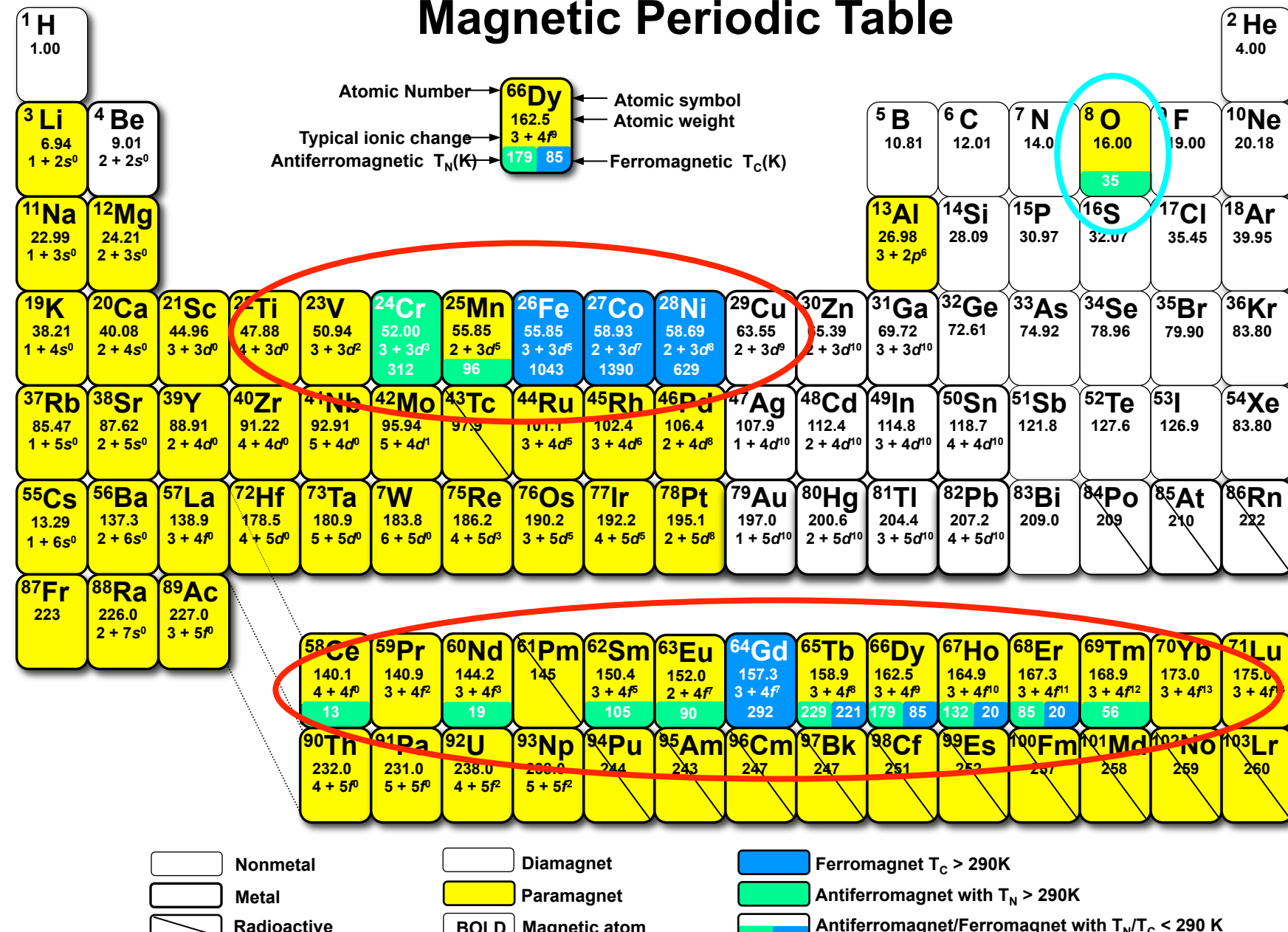
MAGNETISM &
SPIN ELECTRONICS
TRINITY COLLEGE, DUBLIN

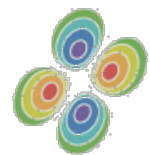
Zug 15-viii-2014



Zug 15-viii-2014

Magnetic Periodic Table





MAGNETISM &
SPIN ELECTRONICS
TRINITY COLLEGE, DUBLIN

Zug 15-viii-2014

Figure 1

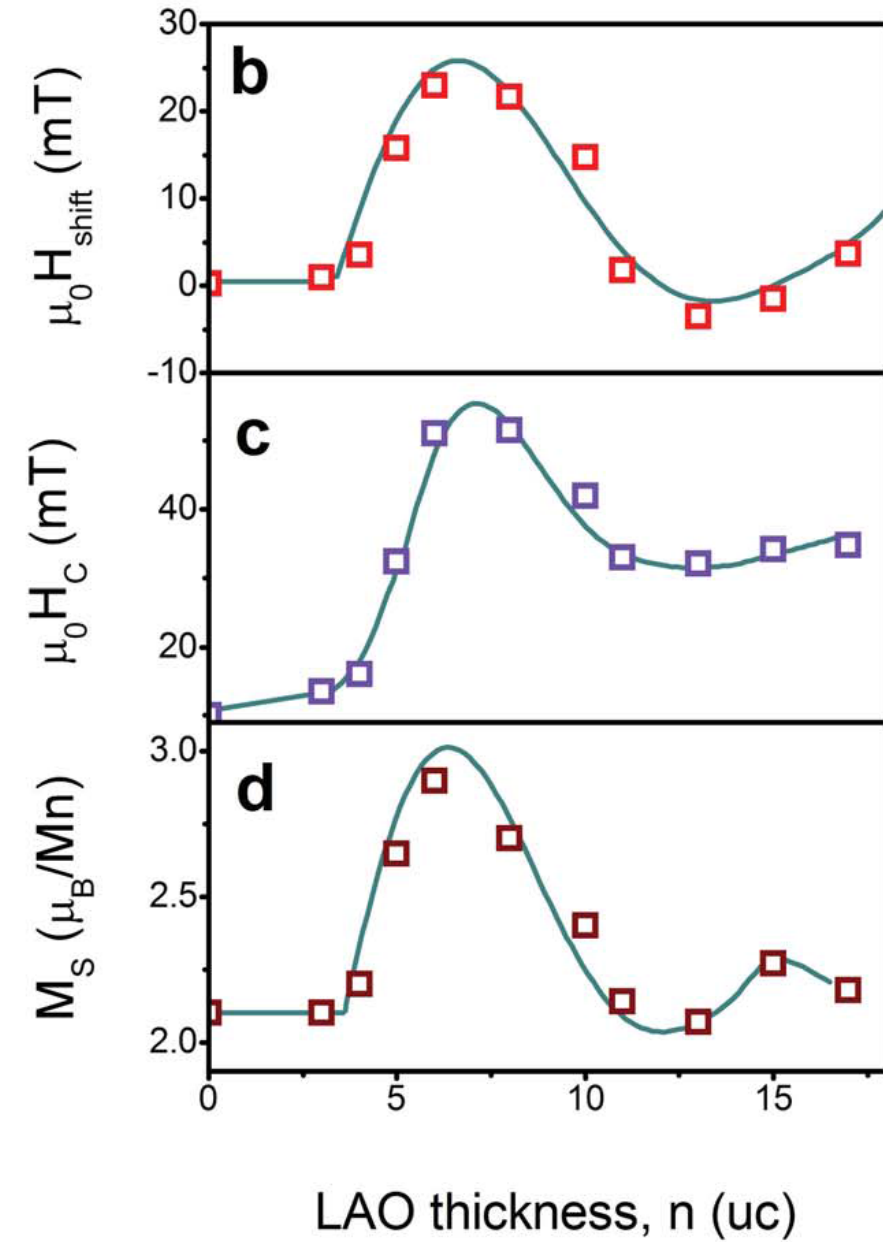
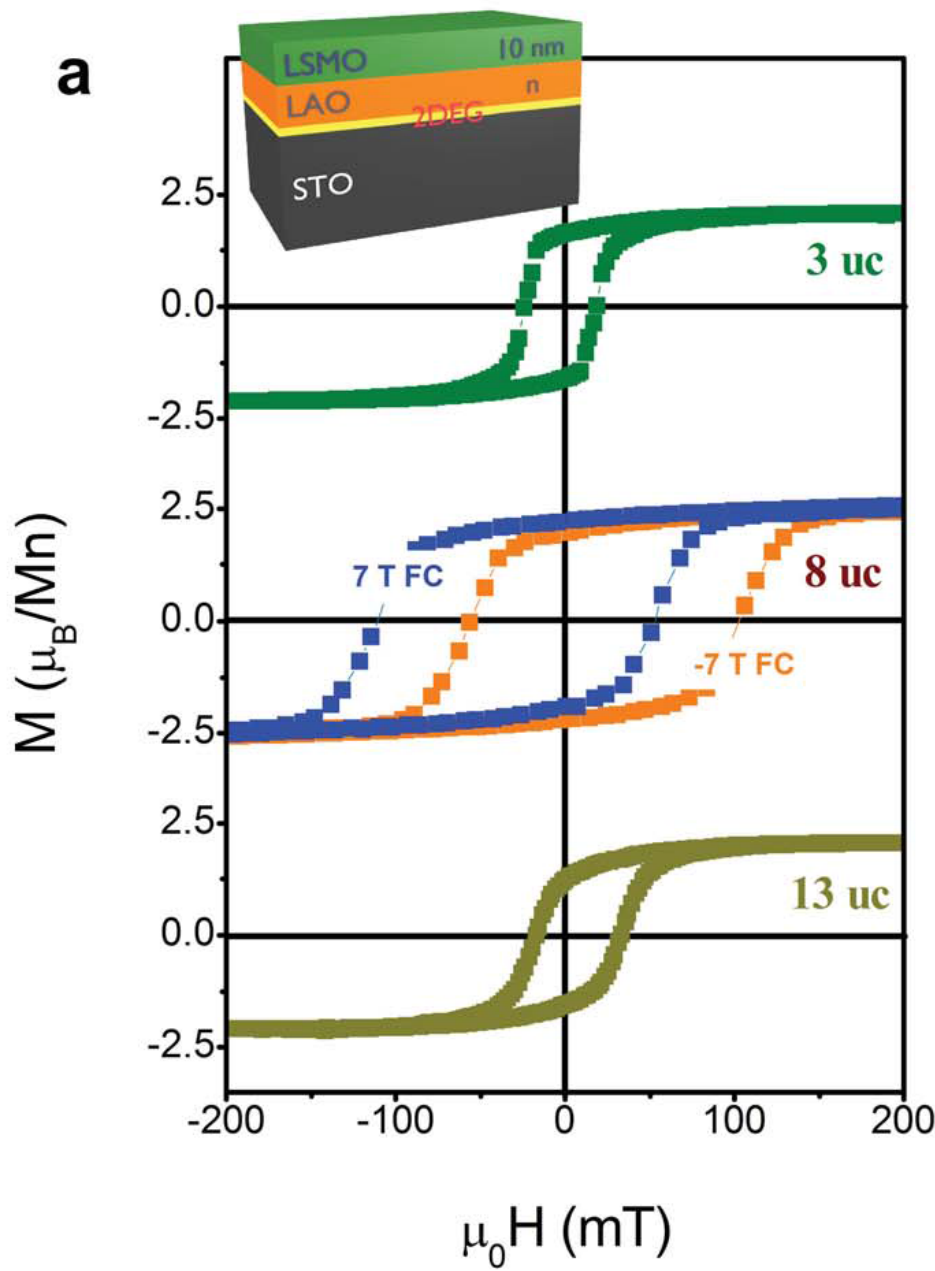


Figure 2

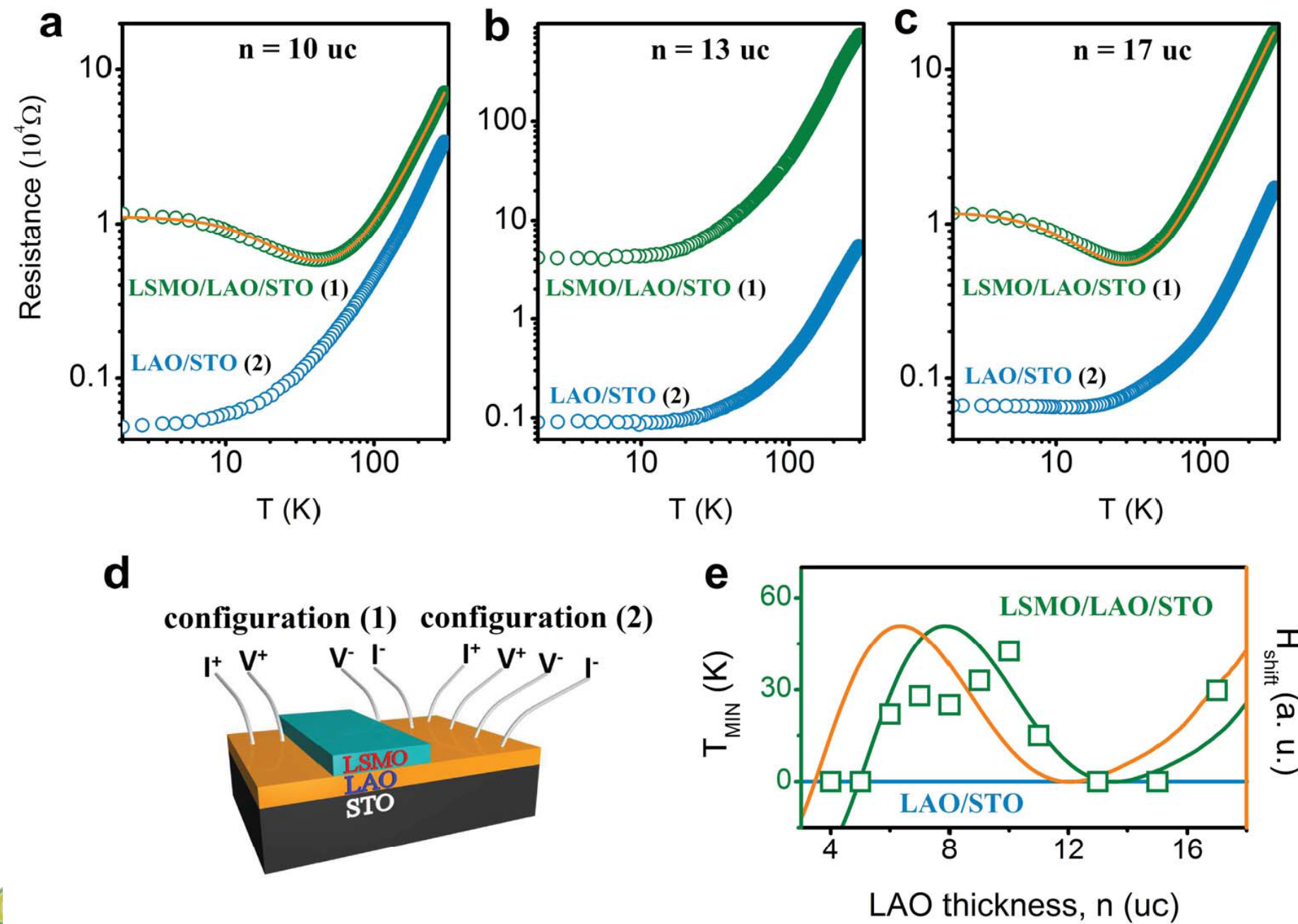


Figure 3

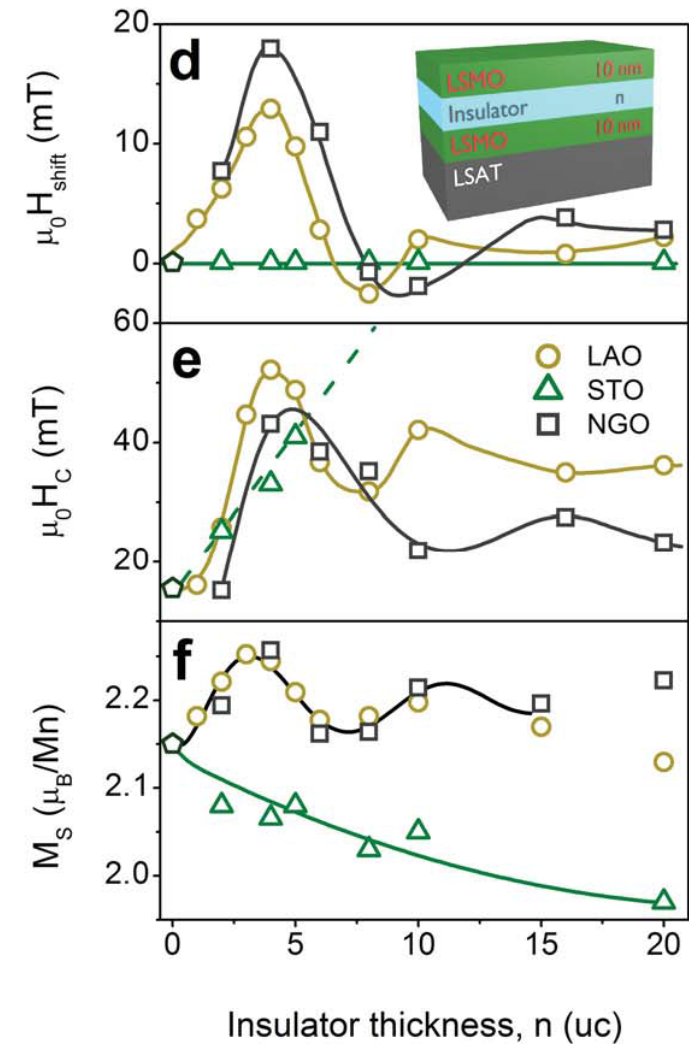
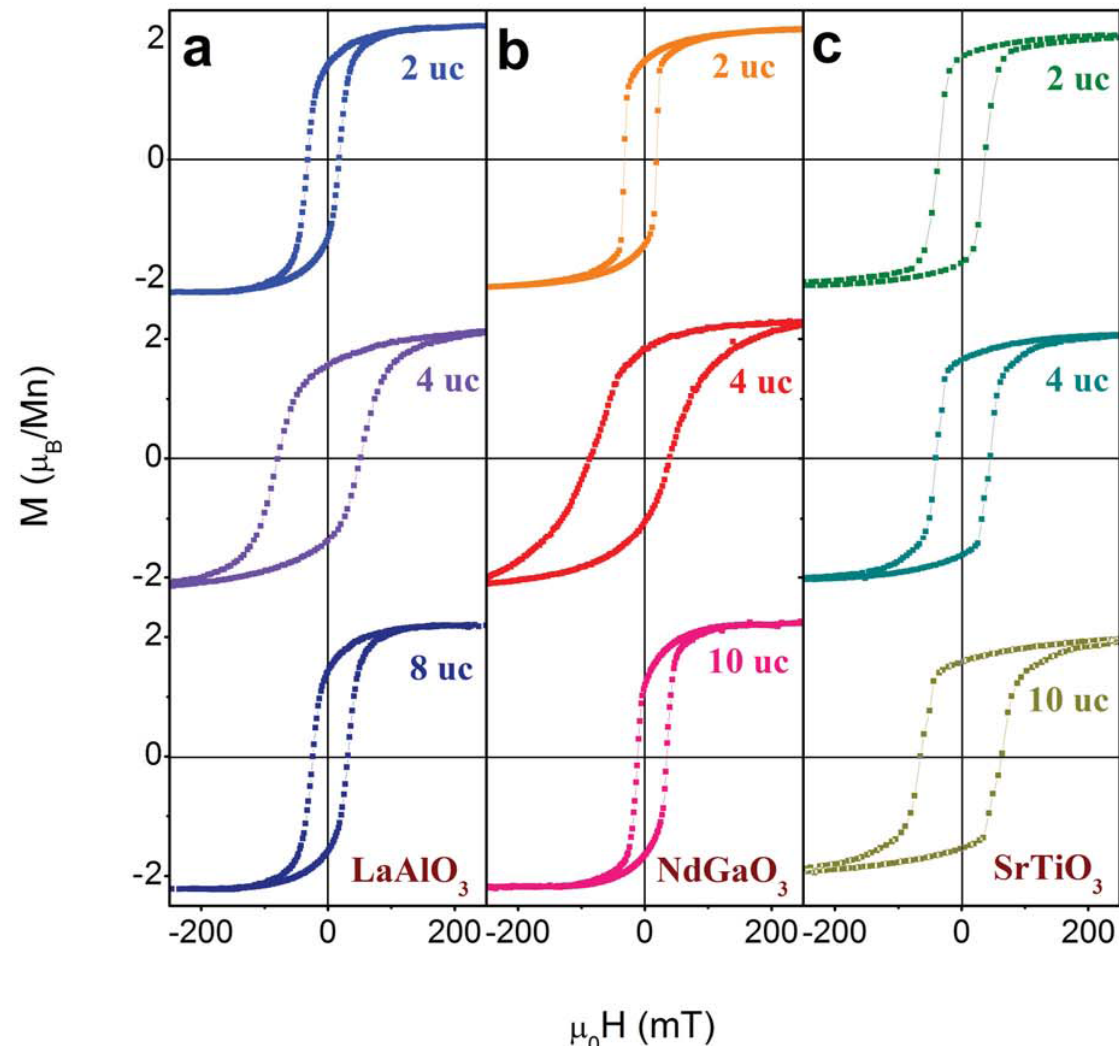


Figure 4

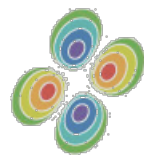
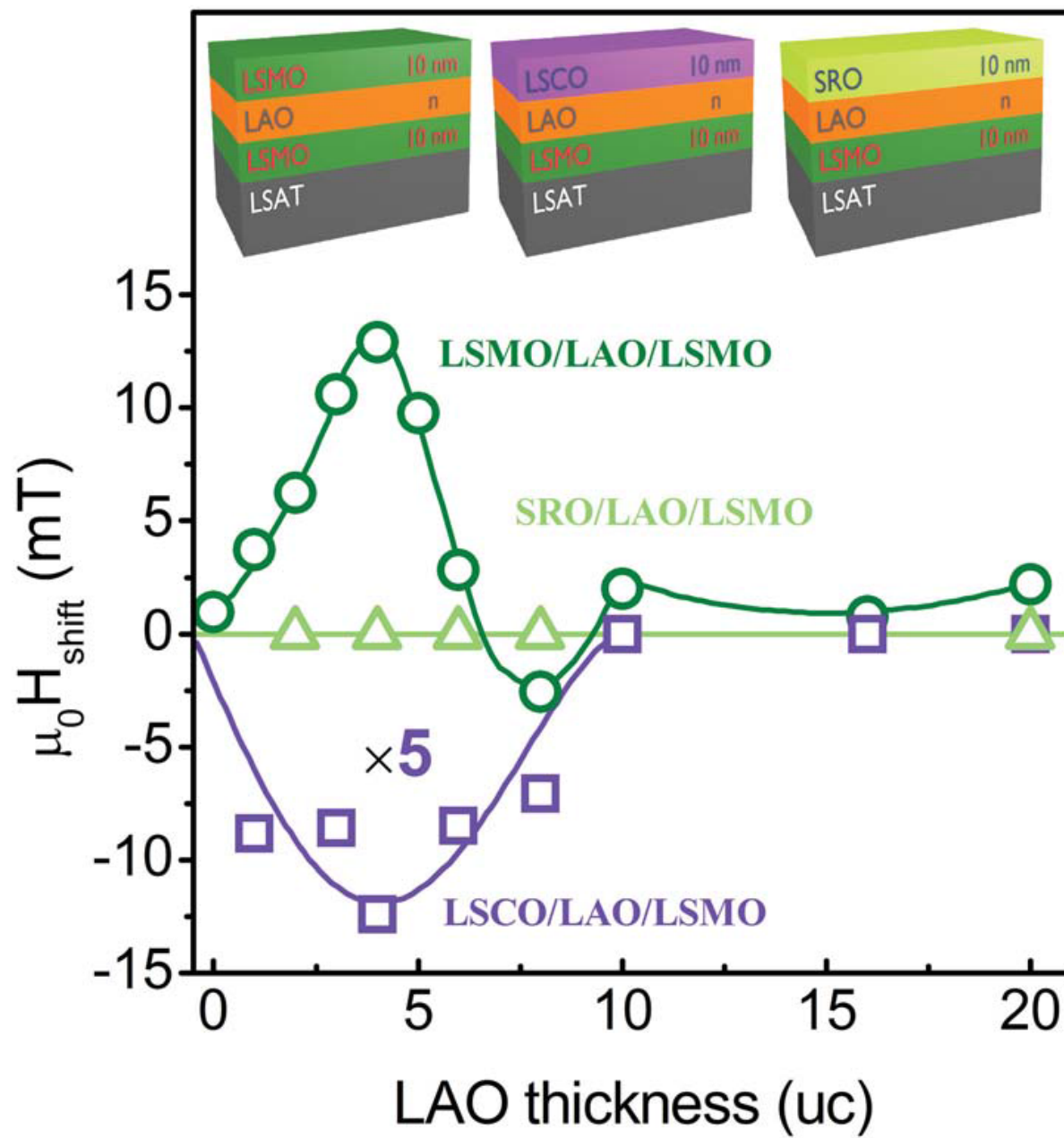
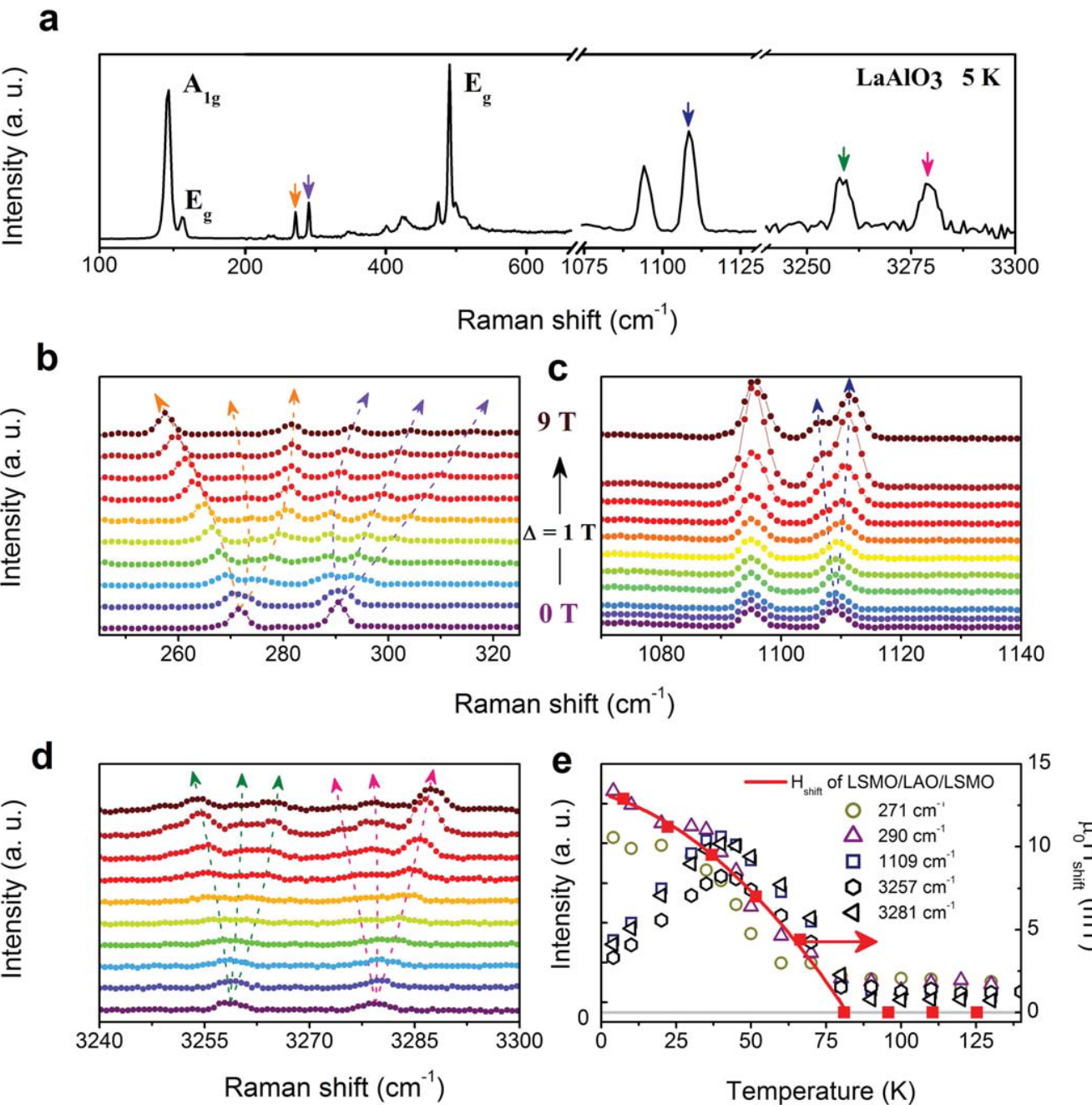
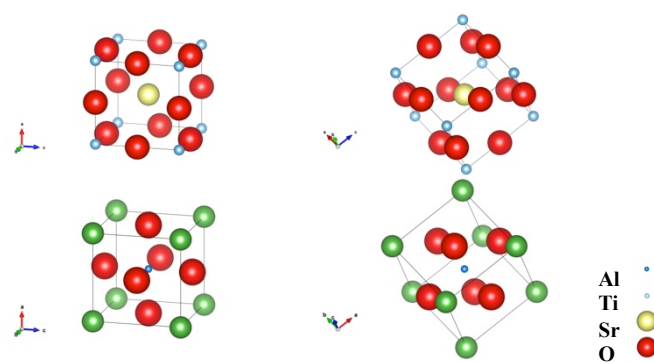


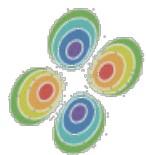
Figure 5





Al
Ti
Sr
O

H Kurt et al PRL 112 027201 (2014)



MAGNETISM &
SPIN ELECTRONICS
TRINITY COLLEGE, DUBLIN

Zug 15-viii-2014

